

UC Berkeley

Research Reports

Title

An Adaption Method For Fuzzy Logic Controllers In Lateral Vehicle Guidance

Permalink

<https://escholarship.org/uc/item/9814b01x>

Authors

Hessburg, Thomas
Tomizuka, Masayoshi

Publication Date

1995

This paper has been mechanically scanned. Some errors may have been inadvertently introduced.

CALIFORNIA PATH PROGRAM
INSTITUTE OF TRANSPORTATION STUDIES
UNIVERSITY OF CALIFORNIA, BERKELEY

An Adaptation Method for Fuzzy Logic Controllers in Lateral Vehicle Guidance

**Thomas Hessburg
Masayoshi Tomizuka**

**California PATH Research Report
UCB-ITS-PRR-95-21**

This work was performed as part of the California PATH Program of the University of California, in cooperation with the State of California Business, Transportation, and Housing Agency, Department of Transportation; and the United States Department of Transportation, Federal Highway Administration.

The contents of this report reflect the views of the authors who are responsible for the facts and the accuracy of the data presented herein. The contents do not necessarily reflect the official views or policies of the State of California. This report does not constitute a standard, specification, or regulation.

June 1995

ISSN 1055-1425

An Adaptation Method for Fuzzy Logic Controllers in Lateral Vehicle Guidance

Thomas Hessburg and Masayoshi Tomizuka

PATH Research Report, MOU 89

June 11, 1995

Keywords: Fuzzy Logic Applications, Fuzzy Logic Control, Lateral Control

Executive Summary

A model reference adaptive fuzzy logic controller (MRAFLC) is designed and simulated for a full-sized test vehicle to achieve control of the lateral motion of the vehicle. The purpose of this research is to design a fuzzy logic controller (based on an *implicit* model of the vehicle) such that changes in operating conditions are addressed in the controller. The changes in operating conditions of interest include vehicle speed and road surface conditions.

The structure of the FLC is modularized as a feedback and *preview* rule base. The parameters of the FLC are tuned automatically using the MRAFLC adaptive tuning scheme. The goal is to make the output of the closed-loop system, under fuzzy logic control, follow a reference output, generated by a fuzzy system. The first step is to define the FLC in a form that enables it to be adjusted on-line. Using Lyapunov theory a *supervisory* control term is constructed such that the closed-loop system under fuzzy logic control will maintain stability in the sense that the states of the vehicle are bounded by a maximum value prescribed by the control designer. An additional Lyapunov analysis is performed to place sufficient conditions on the stability of the adaptation law, ensuring that the output error term is bounded.

The improvement of the performance in lateral motion control in the presence of changing operating conditions using the MRAFLC control design is supported in simulation. A detailed nonlinear model of the vehicle is used for simulation.

Table of Contents

Executive Summary	ii
Table of Contents	iii
List of Figures	iv
1 Introduction	1
2 Stability Analysis	2
3 Adaptive Problem Formulation	9
4 Lyapunov Analysis for Error Convergence.....	15
5 Application to FLC Vehicle Guidance	24
5.1 Feedback Rule Base.....	24
5.2 Preview Rule Base	27
6 MRAFLC Simulation Results for Vehicle Guidance	29
6.1 Feedback Rule Base.....	30
6.2 Preview Rule Base.....	39
7 Conclusion	41
References	42
Appendix A: Membership Definitions.....	43
Appendix B: Linear Model of Vehicle	44

List of Figures

Figure 1: Closed-loop Control Block Diagram	2
Figure 2: Block Diagram of the MRAFLC..	9
Figure 3: V-level Curves	16
Figure 4: V-level Curves; Signal Flow	22
Figure 5: Error bounds	23
Figure 6: Feedback MRAFLC Block Diagram..	24
Figure 7: Preview MRAFLC Block Diagram..	27
Figure 8: Closed-loop Simulation for FLC using x with and without adaptation by MRAFLC, and FSLQ (nominal conditions).	33
Figure 9: Actual Yaw Rate Compared to Model Reference Yaw Rate..	34
Figure 10: Closed-loop Simulation for FLC using x with and without adaptation by MRAFLC with large γ , exhibiting instability..	36
Figure 11: Closed-loop Simulation for FLC using x with and without adaptation by MRAFLC, (high speed)	37
Figure 12: Closed-loop Simulation for FLC using x with and without adaptation by MRAFLC, (slippery road)	38
Figure 13: Simulation Test Track..	39
Figure 14: Closed-loop Simulation for FLC using x with and without adaptation by MRAFLC, and FSLQ/Prev. (nominal conditions).	40

1 Introduction

In this report a formulation is made for a model reference adaptive fuzzy logic control (MRAFLC) algorithm and applied to automatic steering control of a vehicle. The goal is to make the output of the closed-loop system, under fuzzy logic control, follow a reference output, generated by a fuzzy system. This research is an extension of a manually tuned fuzzy logic controller where the theory, design, and experimental results are detailed in [2].

Motivated by a need for a systematic method to generate and modify fuzzy rule based controllers gave rise to learning approaches. This approach began with the self-organizing controller (SOC) [16,17]. The SOC consists of two levels of fuzzy rule bases. The first rule base is the standard fuzzy control rule base, which consists of control inputs in the antecedents (“IF” part) and control outputs in the consequents (“THEN” part). The second level contains a fuzzy rule base consisting of *metu-rules*, which attempt to assess the performance of the closed-loop control system and appropriately modify the standard fuzzy control rule base. Another interesting approach is to conduct learning from information based on an inverse fuzzy model of the open-loop system [8,9]. Several papers propose automated tuning methods for FLCs based on neural networks [3,18], gradient methods [13], and genetic algorithms [4,14]. Although these methods showed improvement over manually tuned FLCs, they usually treat one design stage at a time.

Stable adaptive controllers are well established for continuous system models [6,10,11] and discrete system models [1,12], using Lyapunov’s direct method to ensure stability. With respect to fuzzy control systems, there has been limited research on the stability of such systems [5,7], where the analysis assumes the existence of an explicit mathematical model of the plant to be controlled. In the continuous time domain, an interesting stability analysis was conducted by Wang for adaptive fuzzy controllers for nonlinear systems which requires only parameter bounds of the plant to be controlled [21].

In the following sections the FLC law is defined and stability is discussed for the vehicle modeled with the *linear* model (see appendix B). The control terms generated from the fuzzy rule bases are implemented discretely, but the supervisory control term, constructed such that the states of the vehicle remain bounded, must be implemented

continuously. A method to adapt a FLC in the discrete time domain, following the guidelines of Wang [21], is developed. The objective of this method is to adjust the parameters of an existing FLC for a plant such that the output of the closed-loop control system follows the output of a reference model. Although the linear model of the vehicle is used for the MRAFLC formulation, the explicit parameters of this model are not required for the adaptation. Only bounds on the model parameters are required in order to achieve convergence of the error between the plant output and the model reference output to a lower limit. The model reference output is generated by a fuzzy system. Finally, the theory is supported by simulation results.

2 Stability Analysis

The objective of this section is to establish a condition such that stability of the closed-loop system is achieved in the sense that the state variables are bounded. The control law will be defined in a form that enables its parameters to be adjusted on-line, as discussed in the following section. Then, a coordinate transformation will be performed on the fourth order *linear* model of the vehicle (see appendix B). Using Lyapunov theory, a supervisory control term will be constructed such that the states of the new coordinate system will be shown to be bounded, thus, showing that the states of the linear model are also bounded.

The stability analysis will refer to figure 1.

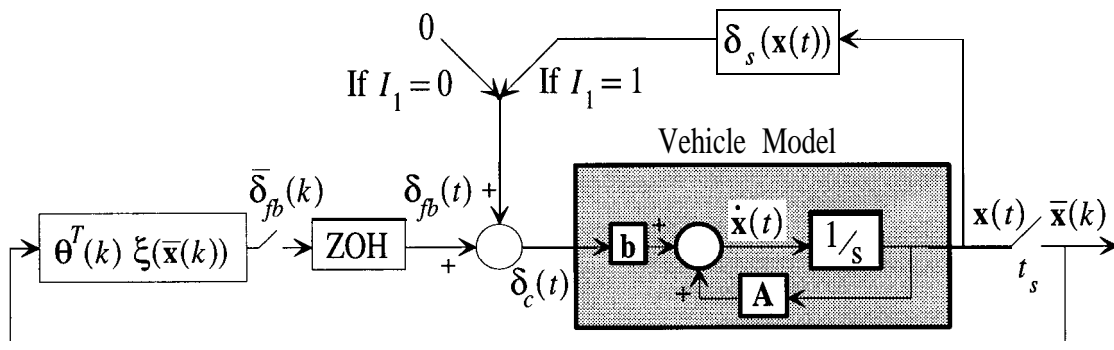


Figure 1: Closed-loop Control Block Diagram

The feedback FLC term can be expressed as

$$\bar{\delta}_{fb}(k) = \theta^T(k) \xi(\bar{\mathbf{x}}(k)) , \quad (1)$$

where $\theta(k) \in \mathfrak{R}^{n_r}$, $\bar{\mathbf{x}}(k) \in \mathfrak{R}^{n_r}$, with n_r as the number of fuzzy rules, and t_s in figure 1 is the sampling time. The choice of this form for $\bar{\delta}_{fb}(k)$ will be made clear in the formulation of the adaptive method in the following section. A zero-order-hold (ZOH) is used to generate $\delta_{fb}(t)$ from $\bar{\delta}_{fb}(k)$. Thus, for $\{t \mid t_s k \leq t < t_s(k+1)\}$, $\delta_{fb}(t) = \bar{\delta}_{fb}(k)$.

The state vector, $x(t)$, for the vehicle is the input to the FLC, given by

$$\mathbf{x}(t) := [x_1, x_2, x_3, x_4]^T := [y_r, \dot{y}_r, \varepsilon - \varepsilon_d, \dot{\varepsilon} - \dot{\varepsilon}_d]^T . \quad (2)$$

The discrete samples of $x(t)$ taken at sample times of t_s , are defined as

$$ii(k) := \mathbf{x}(t_s k) . \quad (3)$$

The goal of stability is to specify an upper bound, M_x , such that the Euclidean norm of $x(t)$ satisfies

$$\|\mathbf{x}(t)\|_2 \leq M_x < \infty . \quad (4)$$

The column vector $\theta(k)$ is defined as

$$\theta(k) := \{\theta_s(k)\}_{s=1}^{n_r} = [\theta_1(k), \theta_2(k), \dots, \theta_{n_r}(k)]^T . \quad (5)$$

The $n_r \times 1$ vector $\theta(k)$ represents the singleton consequent values of each rule (i.e., the s -th element of $\theta(k)$ is the singleton consequent value for the s -th rule). The $n_r \times 1$ function vector, $\bar{\mathbf{x}}(k)$, consists of the information which describes all the membership functions. Using the *linear* vehicle model, each of the four inputs to the FLC is described by five fuzzy subsets or linguistic values. The number of fuzzy rules, n_r , combine multiplicatively and will be $n_r = 5^4 = 625$. Let $\mu_i^s(\bar{x}_i(k))$ denote a membership

function which maps a scalar base variable into a range $[0, 1]$, for the i -th input variable ($i = 1, 2, 3, 4$), and for the s -th rule ($s = 1, \dots, n_r$).

The column function vector $\xi(\bar{\mathbf{x}}(k))$ is defined as

$$\xi(\bar{\mathbf{x}}(k)) := \{\xi_s(\bar{\mathbf{x}}(k))\}_{s=1}^{n_r}, \quad (6)$$

with the fuzzy basis function [20] defined as

$$\xi_s(\bar{\mathbf{x}}(k)) := \frac{\prod_{i=1}^4 \mu_i^s(\bar{x}_i(k))}{\sum_{l=1}^{n_r} \left(\prod_{i=1}^4 \mu_i^l(\bar{x}_i(k)) \right)} \quad \text{for } s = 1, 2, \dots, n_r. \quad (7)$$

The term $\prod_{i=1}^4 \mu_i^s(\bar{x}_i(k))$ in the numerator is the rule *truth* (i.e., the degree to which the s -th rule is true on a scale of $[0, 1]$) of the s -th rule (the t-norm used is the product rule). The denominator is a normalizing factor as it is the summation of all the rule truths.

Note that the following properties can be established:

$$\xi_s(\bar{\mathbf{x}}(k)) \in [0, 1],$$

$$[1, 1, \dots, 1] \xi(\bar{\mathbf{x}}(k)) = 1, \text{ and}$$

$$0 < \xi^T(\bar{\mathbf{x}}(k)) \xi(\bar{\mathbf{x}}(k)) = \|\xi(\bar{\mathbf{x}}(k))\|_2^2 \leq 1. \quad (8)$$

In order to analyze the stability of the system, a model of the vehicle must be defined. The fourth order linearized model developed appendix B without external disturbances chosen for this purpose is described by the following differential equation:

$$\frac{d}{dt} \begin{bmatrix} y_r \\ \dot{y}_r \\ \varepsilon - \varepsilon_d \\ \dot{\varepsilon} - \dot{\varepsilon}_d \end{bmatrix} = \begin{bmatrix} 0 & 1 & 0 & 0 \\ 0 & A_1/v & -A_1 & A_2/v \\ 0 & 0 & 0 & 1 \\ 0 & A_3/v & -A_3 & A_4/v \end{bmatrix} \begin{bmatrix} y_r \\ \dot{y}_r \\ \varepsilon - \varepsilon_d \\ \dot{\varepsilon} - \dot{\varepsilon}_d \end{bmatrix} + \begin{bmatrix} 0 \\ B_1 \\ 0 \\ B_2 \end{bmatrix} \delta_c , \quad (9)$$

or in matrix form

$$\dot{\mathbf{x}} = \mathbf{A}\mathbf{x} + \mathbf{b}\delta_c , \quad (10)$$

where $\mathbf{A} \in \mathfrak{R}^{4 \times 4}$, $\mathbf{b} \in \mathfrak{R}^4$ are defined as in equation (9) and the individual elements are defined in appendix B, with $\mathbf{x}(t)$ defined by equation (2).

Since the 4 x 4 controllability matrix $[\mathbf{b} \ \mathbf{A}\mathbf{b} \ \mathbf{A}^2\mathbf{b} \ \mathbf{A}^3\mathbf{b}]$ is of rank 4, the pair (\mathbf{A}, \mathbf{b}) is controllable and a coordinate transformation can be made such that the system is in controllable canonical form. Thus, there exists a nonsingular matrix, $\mathbf{T} \in \mathfrak{R}^{4 \times 4}$, such that a new coordinate system can be defined as

$$\mathbf{z}(t) := [z_1, z_2, z_3, z_4]^T := \mathbf{T}\mathbf{x}(t) . \quad (11)$$

In the z-coordinate space, the dynamic equations become

$$\dot{\mathbf{z}} = \mathbf{A}_c\mathbf{z} + \mathbf{b}_c\delta_c , \quad (12)$$

where $A_c = \mathbf{TAT}^{-1}$ and $\mathbf{b}_c = \mathbf{Tb}$. Explicitly, \mathbf{A}_c and \mathbf{b}_c are defined as

$$\mathbf{A}_c = \begin{bmatrix} 0 & 1 & 0 & 0 \\ 0 & 0 & 1 & 0 \\ 0 & 0 & 0 & 1 \\ -a_1 & -a_2 & -a_3 & -a_4 \end{bmatrix} \text{ and } \mathbf{b}_c = \begin{bmatrix} 0 \\ 0 \\ 0 \\ b \end{bmatrix}, \quad (13)$$

where $b \in \Re$ and a_i for $i = 1, 2, 3, 4$ are the coefficients of the characteristic polynomial of the open loop plant, defined as

$$\det(s\mathbf{I} - A) = s^4 + a_4s^3 + a_3s^2 + a_2s + a_1. \quad (14)$$

Now the dynamics of the system can be described by the simplified expression

$$z_1^{(4)} = (-a_4z_4 - a_3z_3 - a_2z_2 - a_1z_1) + b\delta_c, \quad (15)$$

where $z_1^{(4)}$ represents the fourth time derivative of z_1 .

Using the vehicle parameters defined in appendix B, the coefficients of equation (15) are computed as:

$$\begin{aligned} a_1 &= a_2 = 0, \\ a_3 &= \frac{4C_s^2(2(l_1^2 + l_2^2) - (l_1 - l_2)^2)}{mI_z v_x^2} + \frac{2C_s(l_2 - l_1)}{I_z}, \text{ and} \\ a_4 &= \frac{2C_s}{v_x} \left(\frac{2}{m} + \frac{l_1^2 + l_2^2}{I_z} \right). \end{aligned} \quad (16)$$

The function $f(\mathbf{z}(t))$ is defined to be

$$f(\mathbf{z}(t)) = -\frac{2C_s}{v_x} \left(\frac{2}{m} + \frac{l_1^2 + l_2^2}{I_z} \right) z_4 - \left(\frac{4C_s^2(2(l_1^2 + l_2^2) - (l_1 - l_2)^2)}{mI_z v_x^2} + \frac{2C_s(l_2 - l_1)}{I_z} \right) z_3. \quad (17)$$

Thus, the dynamic equation becomes

$$z_1^{(4)} = f(\mathbf{z}(t)) + b\delta_c . \quad (18)$$

Let a Lyapunov function candidate be defined as

$$V(\mathbf{z}(t)) := \frac{1}{2} \mathbf{z}(t)^T \mathbf{z}(t) = \frac{1}{2} \|\mathbf{z}(t)\|_2^2 \quad (19)$$

or

$$V(\mathbf{z}(t)) = \frac{1}{2} (z_1^2 + z_2^2 + z_3^2 + z_4^2) . \quad (20)$$

Differentiating with respect to time yields

$$\dot{V}(\mathbf{z}(t)) = z_1 z_2 + z_2 z_3 + z_3 z_4 + z_4 (f(\mathbf{z}(t)) + b\delta_c) \quad (21)$$

and the following inequality can be established:

$$\dot{V}(\mathbf{z}(t)) \leq |z_1 z_2| + |z_2 z_3| + |z_3 z_4| + |z_4 f(\mathbf{z}(t))| + |z_4 b \delta_{fb}(t)| + z_4 b \delta_s(\mathbf{x}(t)) , \quad (22)$$

where the substitution $\delta_c = \delta_{fb}(t) + \delta_s(\mathbf{x}(t))$ has been made (i.e., the input, δ_c , to the vehicle has a feedback FLC control term, $\delta_{fb}(t)$, and a *supervisory* control term, $\delta_s(\mathbf{x}(t))$).

The next step is to construct a supervisory control term, $\delta_s(\mathbf{x}(t))$, such that if $\mathbf{x}(t)$ ever reaches a boundary specified by $\|\mathbf{x}(t)\|_2 \leq M_x$, then $\dot{V} \leq 0$ is always maintained, keeping $\mathbf{x}(t)$ from going beyond this boundary. In order to accomplish this, some knowledge about the parameter uncertainty bounds of the vehicle is required. Specifically, an upper bound function, $f^U(\mathbf{z}(t))$, such that $|f(\mathbf{z}(t))| \leq f^U(\mathbf{z}(t))$, and a lower bound constant, b_L , such that $0 < b_L \leq b$, must be known. Since $f(\mathbf{z}(t))$ and b are functions of vehicle parameters, the precise values for the function, $f^U(\mathbf{z}(t))$, and the constant, b , can be determined by using the extreme values of the vehicle parameters (i.e., of m, I_2, C_s, l_1, l_2 , and v_x), such that $|f(\mathbf{z}(t))| \leq f^U(\mathbf{z}(t))$ and $0 < b_L \leq b$ are satisfied.

Thus, knowing that $b_L > 0$ and $z(t) = \mathbf{T}\mathbf{x}(t)$, and assuming that $|z_4| \neq 0$, let the supervisory control, $\delta_s(\mathbf{x}(t))$, be defined as

$$\delta_s(\mathbf{x}(t)) = -I_1 \text{sgn}(z_4) \left(\left| \delta_{fb}(t) \right| + \frac{|z_1 z_2| + |z_2 z_3|}{|z_4| b_L} + \frac{|z_3| + |f^U(\mathbf{z}(t))|}{b_L} \right), \quad (23)$$

where, for a specified constant \bar{V} , I_1 is defined as

$$I_1 = \begin{cases} 1; & \text{if } V(\mathbf{z}(t)) \geq \bar{V} \\ 0; & \text{if } V(\mathbf{z}(t)) < \bar{V} \end{cases}. \quad (24)$$

Examining $\dot{V}(\mathbf{z}(t))$ for the case of $I_1 = 1$ yields

$$\begin{aligned} \dot{V}(\mathbf{z}(t)) &\leq |z_1 z_2| + |z_2 z_3| + |z_3 z_4| + |z_4 f(\mathbf{z}(t))| + |z_4 b \delta_{fb}(t)| \\ &\quad - |z_4 b \delta_{fb}(t)| - \frac{b}{b_L} (|z_1 z_2| + |z_2 z_3| + |z_3 z_4| + |z_4 f^U(\mathbf{z}(t))|) \end{aligned} \quad (25)$$

or

$$\dot{V}(\mathbf{z}(t)) \leq 0. \quad (26)$$

This ensures that if the initial conditions of \mathbf{z} are such that $V(\mathbf{z}(0)) \leq \bar{V}$, then $V(\mathbf{z}(t)) \leq \bar{V}$ for all time. Thus, $\|\mathbf{z}(t)\|_2$ is bounded, and therefore $\|\mathbf{x}(t)\|_2 = \|\mathbf{T}^{-1}\mathbf{z}(t)\|_2$ is bounded. If $M_x c \infty$ is specified to achieve $\|\mathbf{x}(t)\|_2 \leq M_x$, then this condition is ensured if we take \mathbf{T} (which is in terms of vehicle parameters m, I_z, C_s, l_1, l_2 , and v_x) and choose extreme values of the vehicle parameters to obtain a \mathbf{T}_e such that $\lambda_{\min}((\mathbf{T}_e^{-1})^T \mathbf{T}_e^{-1}) \leq \lambda_{\min}((\mathbf{T}^{-1})^T \mathbf{T}^{-1})$ for all \mathbf{T} . Then we must maintain $\mathbf{z}(t)$ such that $\|\mathbf{z}(t)\|_2 \leq (\lambda_{\min}((\mathbf{T}_e^{-1})^T \mathbf{T}_e^{-1}))^{\frac{1}{2}} M_x$, where $\lambda_{\min}(\mathbf{Q})$ denotes the minimum eigenvalue of the square matrix, \mathbf{Q} . Thus, in the above formulation, \bar{V} must be chosen such that $\bar{V} = \lambda_{\min}((\mathbf{T}_e^{-1})^T \mathbf{T}_e^{-1}) M_x^2$. The assumption that $|z_4| \neq 0$, is a valid assumption (except for a set with zero measure) since $\delta_s(\mathbf{x}(t))$ will only be implemented when $\|\mathbf{z}(t)\|_2 = \|\mathbf{T}\mathbf{x}(t)\|_2 = \sqrt{\lambda_{\min}((\mathbf{T}^{-1})^T \mathbf{T}^{-1})} M_x$, and since z_4 is a linear combination of $\mathbf{x}(t)$, where $\mathbf{x}(t) \neq \mathbf{0}$, z_4 will never be zero over a finite time interval.

In order for this stability condition to be satisfied, the supervisory control term, $\delta_s(\mathbf{x}(t))$, must be implemented continuously. Although the FLC feedback control term in the time domain, $\delta_{fb}(t)$, will jump due to the ZOH of the discrete implementation, the states $\mathbf{x}(t)$ will remain continuous. Thus, the construction of $\delta_s(\mathbf{x}(t))$ using Lyapunov theory is valid.

3 Adaptive Problem Formulation

The block diagram in figure 2 shows the flow of signals for the model reference adaptive fuzzy logic controller (MRAFLC). In the following section each block in the diagram will be defined under the assumption that the physical plant to be controlled is the vehicle modeled by the *linear* model (see appendix B). It should be noted that states of the linear model will remain bounded by the continuous implementation of the supervisory control term, $\delta_s(\mathbf{x}(t))$, as described in the previous section.

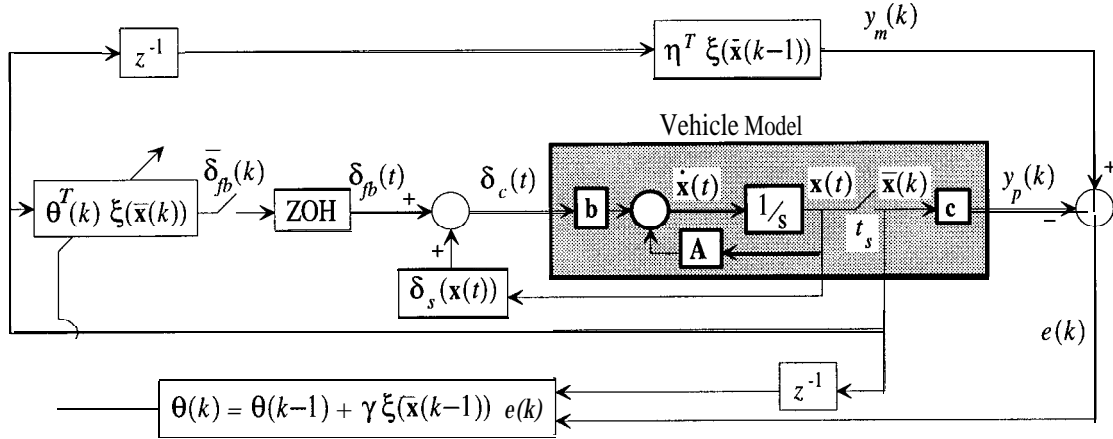


Figure 2: Block Diagram of the MRAFLC

The purpose of the next analysis will be to derive an expression for the incremental propagation of the state sequence, $\bar{\mathbf{x}}(k)$, according to the above figure. Since the linear system is described by $\dot{\mathbf{x}} = \mathbf{A}\mathbf{x} + \mathbf{b}\delta_c$, given by equation (10), the solution of $\mathbf{x}(t)$ can be written as

$$\mathbf{x}(t) = e^{\mathbf{A}t}\mathbf{x}(0) + e^{\mathbf{A}t} \int_0^t e^{-\mathbf{A}\tau} \mathbf{b} \delta_c(\tau) d\tau . \quad (27)$$

Thus, the following two solutions can be written for consecutive samples of $\mathbf{x}(t)$:

$$\mathbf{x}(t_s k) = e^{A t_s k} \mathbf{x}(0) + e^{A t_s k} \int_0^{t_s k} e^{-A \tau} \mathbf{b} \delta_c(\tau) d\tau \quad \text{and} \quad (28)$$

$$\mathbf{x}(t_s(k+1)) = e^{A t_s(k+1)} \mathbf{x}(0) + e^{A t_s(k+1)} \int_0^{t_s(k+1)} e^{-A \tau} \mathbf{b} \delta_c(\tau) d\tau \quad . \quad (29)$$

Multiplying both sides of equation (28) by $e^{A t_s}$ and subtracting the result from equation (29) yields, after some manipulation,

$$\mathbf{x}(t_s(k+1)) = e^{A t_s} \mathbf{x}(t_s k) + e^{A t_s(k+1)} \int_{t_s k}^{t_s(k+1)} e^{-A \tau} \mathbf{b} \delta_c(\tau) d\tau \quad (30)$$

or

$$\mathbf{x}(t_s(k+1)) = e^{A t_s} \mathbf{x}(t_s k) + \int_{t_s k}^{t_s(k+1)} e^{A(t_s(k+1)-\tau)} \mathbf{b} \delta_c(\tau) d\tau \quad . \quad (31)$$

By a suitable choice for a change of variables, $\sigma = t_s(k+1) - \tau$, the integral term can be modified to form

$$\mathbf{x}(t_s(k+1)) = e^{A t_s} \mathbf{x}(t_s k) + \int_0^{t_s} e^{A \sigma} \mathbf{b} \delta_c(t_s(k+1) - \sigma) d\sigma \quad . \quad (32)$$

Since δ_c has two components, $\delta_c(t) = \delta_{fb}(t) + \delta_s(\mathbf{x}(t))$, and for $\delta_{fb}(t) = \delta_{fb}(t_s k)$ for $\{t \mid t_s k \leq t < t_s(k+1)\}$ from the ZOH, we have

$$\mathbf{x}(t_s(k+1)) = e^{A t_s} \mathbf{x}(t_s k) + \left(\int_0^{t_s} e^{A \sigma} \mathbf{b} d\sigma \right) \delta_{fb}(t_s k) + \int_0^{t_s} e^{A \sigma} \mathbf{b} \delta_s(t_s(k+1) - \sigma) d\sigma \quad . \quad (33)$$

Let $\bar{\mathbf{A}}$ and $\bar{\mathbf{b}}$ be defined such that

$$\bar{\mathbf{A}} := e^{A t_s} \quad \text{and} \quad \bar{\mathbf{b}} := \int_0^{t_s} e^{A \sigma} \mathbf{b} d\sigma \quad . \quad (34)$$

The model of the plant to be controlled can be expressed as a propagation of a sequence, $E(k)$, where the sampling time is t_s , and noting that $\bar{\delta}_{fb}(k) = \delta_{fb}(t_s k)$,

$$\bar{\mathbf{x}}(k+1) = \bar{\mathbf{A}}\bar{\mathbf{x}}(k) + \bar{\mathbf{b}}\bar{\delta}_{fb}(k) + \int_0^{t_s} e^{A\sigma} \mathbf{b} \delta_s(t_s(k+1) - \sigma) d\sigma \quad \text{and} \quad (35)$$

$$y_p(k) = \mathbf{c}\bar{\mathbf{x}}(k), \quad (36)$$

where $\bar{\mathbf{A}} \in \mathfrak{R}^{4 \times 4}$, $\bar{\mathbf{b}} \in \mathfrak{R}^4$, $\mathbf{c} \in \mathfrak{R}^4$, and $\bar{\mathbf{x}}(k) \in \mathfrak{R}^4$, $y_p(k) \in \mathfrak{R}$.

The terminology for the coefficients of $\bar{\mathbf{A}}$, $\bar{\mathbf{b}}$, and \mathbf{c} are defined as

$$\bar{\mathbf{A}} := \{\bar{A}_{ij}\} \quad (\text{i-th row for } i = 1, 2, 3, 4, \text{ and j-th column for } i = 1, 2, 3, 4),$$

$$\bar{\mathbf{b}}^T := [\bar{b}_1, \bar{b}_2, \bar{b}_3, \bar{b}_4], \quad \text{and}$$

$$\mathbf{c} := [0, 0, 0, 1], \quad (37)$$

where \bar{b}_i , and \bar{A}_{ij} are scalars which depend on the vehicle parameters and operating conditions.

The sampled state vector for the vehicle is given by

$$\bar{\mathbf{x}}(k) := \begin{bmatrix} \bar{x}_1(k) \\ \bar{x}_2(k) \\ \bar{x}_3(k) \\ \bar{x}_4(k) \end{bmatrix} := \begin{bmatrix} y_r(t_s k) \\ \dot{y}_r(t_s k) \\ \epsilon(t_s k) - \epsilon_d(t_s k) \\ \dot{\epsilon}(t_s k) - \dot{\epsilon}_d(t_s k) \end{bmatrix}. \quad (38)$$

Recall that the feedback controller can be expressed as

$$\bar{\delta}_{fb}(k) = \theta^T(k) \xi(\bar{\mathbf{x}}(k)), \quad (39)$$

where $\theta(k) \in \mathfrak{R}^{n_r}$, $\xi(\bar{\mathbf{x}}(k)) \in \mathfrak{R}^{n_r}$, and n_r is the number of fuzzy rules.

The adjustable column vector $\delta(k)$ is defined by equation (5), and the function vector $\xi(\bar{\mathbf{x}}(k))$ is defined by Eqns. (6) and (7). The membership functions are assumed to be fixed during adaptation. Therefore, the vector $\xi(\bar{\mathbf{x}}(k))$ is not adapted in this formulation. The purpose of adapting $\theta(k)$ and not adapting $\xi(\bar{\mathbf{x}}(k))$ will be clear in the Lyapunov analysis where we show the convergence of the output errors to a lower limit in the MRAFLC.

The reference model is given by a fuzzy system, where n_r is the number of fuzzy rules, as

$$y_r(k) := \boldsymbol{\eta}^T \xi(\bar{\mathbf{x}}(k-1)), \quad (40)$$

where $y_r(k) \in \mathfrak{R}$, $\xi(\bar{\mathbf{x}}(k))$ is defined as in Eqns. (6) and (7). The fuzzy system for the reference model and the fuzzy system for control have the same input variables. Furthermore, the function vector, $\xi(\bar{\mathbf{x}}(k))$, and thus, the membership functions of the two fuzzy systems are the same. This enables the algorithm to pinpoint which rules, along with their respective firing strengths, are responsible for the error in output.

The column vector $\boldsymbol{\eta}$ is defined as

$$\boldsymbol{\eta} := \{\eta_s\}_{s=1}^{n_r}. \quad (41)$$

The model is designed by the control engineer. In the case of lateral motion control, the designer considers a state of the vehicle one step in the past (i.e., at $\bar{\mathbf{x}}(k-1)$) and decides on the proper motion of the vehicle in terms of the yaw rate. The designer adjusts the consequent parameters, $\boldsymbol{\eta}$, such that a reference yaw rate is inferred from the past state of the vehicle. Thus, the designer formulates a linguistic reference model, incorporating such aspects as rise-time and damping, as well as strategy regarding how the human would like the motion of the vehicle to move in order to address ride quality.

Suppose there exists a control sequence $\delta^*(k)$, (an ideal control sequence), such that with control commands coming *only* from the FLC (i.e., $\delta_s(\mathbf{x}(t)) = 0$ for $\{t \mid t_s k \leq t < t_s(k+1)\}$), $y_p(k+1) = y_m(k+1)$. Then, we have from Eqns. (35), (36), and (40)

$$y_p(k+1) = \mathbf{c}(\bar{\mathbf{A}}\mathbf{x}(k) + \bar{\mathbf{b}}\delta^*(k)) = \eta^T \xi(\bar{\mathbf{x}}(k)) = y_m(k+1) . \quad (42)$$

Note by equation (37) we have

$$\mathbf{c}\bar{\mathbf{b}} = \bar{b}_4 . \quad (43)$$

Recalling the definition of an element of the i-th row and j-th column of $\bar{\mathbf{A}}$ as $\bar{\mathbf{A}}_{ij}$, we have

$$\mathbf{c}\bar{\mathbf{A}} = [\bar{A}_{41}, \bar{A}_{42}, \bar{A}_{43}, \bar{A}_{44}] . \quad (44)$$

Substituting Eqns. (43) and (44) into equation (42) and solving for $\delta^*(k)$, we have

$$\delta^*(k) = \frac{\eta^T \xi(\bar{\mathbf{x}}(k)) - \sum_{i=1}^4 \bar{A}_{4i} \bar{x}_i}{\bar{b}_4} \quad (45)$$

where $\bar{b}_4 > 0$.

Since the definitions of the membership functions, $\mu_i^s(\bar{x}_i(k))$, and thus, $\xi(\bar{\mathbf{x}}(k))$, are fixed, the only adjustable parameter in the controller, equation (39), is $\delta(k)$. For analytic purposes, we make a definition for the best choice of the parameter vector θ as θ^* , by the following:

$$\theta^* := \arg \min_{\theta \mid \|\theta\|_2 \leq M_\theta} \left[\sup_{\bar{\mathbf{x}} \mid \|\bar{\mathbf{x}}\|_2 \leq M_x} |\theta^T \xi(\bar{\mathbf{x}}) - \delta^*| \right] . \quad (46)$$

The choice of M_θ , can be considered a constraint on the desired control law (i.e., $\|\theta^*\|_2 \leq M_\theta < \infty$) and is determined by the designer.

Also, we define the *minimum approximation error* [21] as:

$$w(k) := (\theta^*)^T \xi(\bar{\mathbf{x}}(k)) - \delta^*(k). \quad (47)$$

For analytic purposes, an upper bound on the magnitude of $w(k)$ is denoted as w^U , defined such that

$$w^U \geq \sup_{\bar{\mathbf{x}} \mid \|\bar{\mathbf{x}}\|_2 \leq M_x} |\xi(\bar{\mathbf{x}})|. \quad (48)$$

The term w^U represents the “worst case” resolution of the FLC. Theoretically, the term w^U can be made as small as desired by increasing the number of fuzzy subsets which describe each linguistic variable, and thus, increasing the number of rules [19].

Using the control law of equation (39), the actual plant output becomes (see Eqns. (35) and (36))

$$y_p(k+1) = \mathbf{c} \left(\bar{\mathbf{A}}\mathbf{x}(k) + \bar{\mathbf{b}}\theta^T(k)\xi(\bar{\mathbf{x}}(k)) + \int_0^{t_s} e^{\mathbf{A}\sigma} \mathbf{b} \delta_s(t_s(k+1) - \sigma) d\sigma \right). \quad (49)$$

Having defined the propagation of $y_m(k)$ and $y_p(k)$, the next step is to form an expression for the error propagation. An error equation is defined using Eqns. (40) and (49) as

$$\begin{aligned} e(k+1) &:= y_m(k+1) - y_p(k+1) \\ &= \eta^T \xi(\bar{\mathbf{x}}(k)) - \mathbf{c} \left(\bar{\mathbf{A}}\mathbf{x}(k) + \bar{\mathbf{b}}\theta^T(k)\xi(\bar{\mathbf{x}}(k)) + \int_0^{t_s} e^{\mathbf{A}\sigma} \mathbf{b} \delta_s(t_s(k+1) - \sigma) d\sigma \right). \end{aligned} \quad (50)$$

We add and subtract $\delta^*(k)$ to get

$$\begin{aligned} e(k+1) &= \eta^T \xi(\bar{\mathbf{x}}(k)) - \\ &\mathbf{c} \left(\bar{\mathbf{A}}\mathbf{x}(k) + \bar{\mathbf{b}} \left(\theta^T(k)\xi(\bar{\mathbf{x}}(k)) + \int_0^{t_s} e^{\mathbf{A}\sigma} \mathbf{b} \delta_s(t_s(k+1) - \sigma) d\sigma - \delta^*(k) + \delta^*(k) \right) \right) \end{aligned} \quad (51)$$

or

$$\begin{aligned}
e(k+1) &= \eta^T \xi(\bar{\mathbf{x}}(k)) - c\delta(k) \\
&\quad - \mathbf{c}\bar{\mathbf{b}}\theta^T(k)\xi(\bar{\mathbf{x}}(k)) + \mathbf{c} \int_0^{t_s} e^{A\sigma} \mathbf{b} \delta_s(t_s(k+1) - \sigma) d\sigma + \mathbf{c}\bar{\mathbf{b}}\delta^*(k) - \mathbf{c}\bar{\mathbf{b}}\delta^*(k).
\end{aligned} \tag{52}$$

Using equation (47) to eliminate the first occurrence of $\delta^*(k)$, we get

$$\begin{aligned}
e(k+1) &= \eta^T \xi(\bar{\mathbf{x}}(k)) - \mathbf{c}\bar{\mathbf{A}}\bar{\mathbf{x}}(k) - \mathbf{c}\bar{\mathbf{b}}(\theta(k) - \theta^*)^T \xi(\bar{\mathbf{x}}(k)) + \\
&\quad \mathbf{c} \int_0^{t_s} e^{A\sigma} \mathbf{b} \delta_s(t_s(k+1) - \sigma) d\sigma - \mathbf{c}\bar{\mathbf{b}}w(k) - \mathbf{c}\bar{\mathbf{b}}\delta^*(k).
\end{aligned} \tag{53}$$

Substituting $\delta^*(k)$ from equation (45), and noting Eqns. (43) and (44), we have

$$\begin{aligned}
e(k+1) &= \eta^T \xi(\bar{\mathbf{x}}(k)) - \mathbf{c}\bar{\mathbf{A}}\bar{\mathbf{x}}(k) - \bar{b}_4(\theta(k) - \theta^*)^T \xi(\bar{\mathbf{x}}(k)) \\
&\quad + \mathbf{c} \int_0^{t_s} e^{A\sigma} \mathbf{b} \delta_s(t_s(k+1) - \sigma) d\sigma - \bar{b}_4 w(k) - \eta^T \xi(\bar{\mathbf{x}}(k)) + \mathbf{c}\bar{\mathbf{A}}\bar{\mathbf{x}}(k).
\end{aligned} \tag{54}$$

Canceling terms and defining the vector $\phi(k) := \theta^* - \delta(k)$, we get the final expression for the propagation of the error,

$$e(k+1) = \bar{b}_4 \phi^T(k) \xi(\bar{\mathbf{x}}(k)) - \bar{b}_4 w(k) + \mathbf{c} \int_0^{t_s} e^{A\sigma} \mathbf{b} \delta_s(t_s(k+1) - \sigma) d\sigma. \tag{55}$$

Note that if the closed-loop system satisfies $\|\mathbf{x}(t)\|_2 < M_x$ for $\{t \mid t_s k \leq t < t_s(k+1)\}$, then $\delta_s(\mathbf{x}(t)) = 0$ for $\{t \mid t_s k \leq t < t_s(k+1)\}$, and the error propagation term simplifies to

$$e(k+1) = \bar{b}_4 \phi^T(k) \xi(\bar{\mathbf{x}}(k)) - \bar{b}_4 w(k). \tag{56}$$

4 Lyapunov Analysis for Error Convergence

The purpose of this Lyapunov Analysis is to show that the magnitude of the output error term approaches a positive lower limit, e_L , specified by the control designer.

Furthermore, a condition is placed on γ , a positive scalar parameter which determines the rate of adaptation.

The analysis begins by defining a Lyapunov function candidate to include an output error term, $e(k)$, and an error term between the “best choice” for the consequent vector and the actual consequent vector, $\phi(k) := \theta^* - \delta(k)$,

$$V(k) := e^2(k) + \frac{\phi^T(k)\phi(k)}{\gamma} = e^2(k) + \frac{1}{\gamma}\|\phi(k)\|_2^2. \quad (57)$$

This Lyapunov function can be graphically visualized by V-level curves in figure 3. A lower limit on $e(k)$ is specified by the control designer denoted as e_L . The role of e_L is that adaptation only occurs when $|e(k)| > e_L$. The assumption is that if $|e(k)| \leq e_L$, then the closed-loop produces an output close enough to the reference model output to satisfy design specifications. The only restriction on e_L is that it be larger than the component of the output error term due to the limit on the degree of resolution of the fuzzy system used for control. In other words, using a FLC to approximate an optimal control sequence, $\delta^*(k)$, we cannot expect to achieve error terms smaller than what the resolution of the FLC will allow. This analysis will investigate what happens to $V(k)$ when $|e(k)| > e_L$.

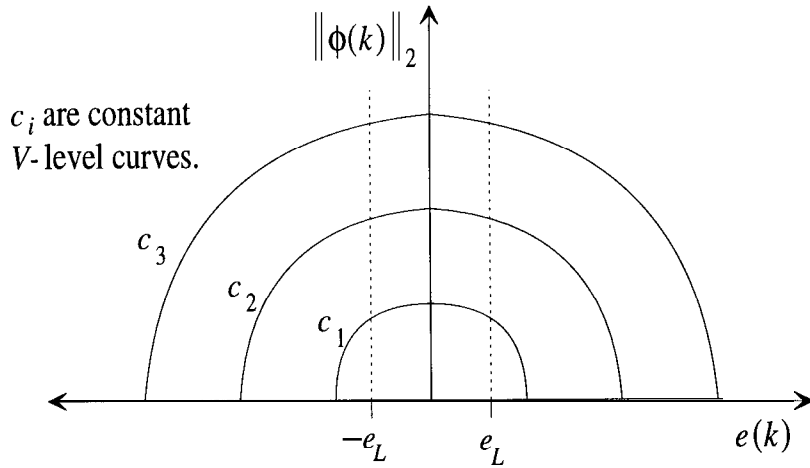


Figure 3: V-level Curves

The forward difference function, $\Delta V(k) := V(k+1) - V(k)$, becomes

$$\Delta V(k) = e^2(k+1) + \frac{\phi^T(k+1)\phi(k+1)}{\gamma} - e^2(k) - \frac{\phi^T(k)\phi(k)}{\gamma} . \quad (58)$$

The following *adaptation law* is proposed:

$$\phi(k+1) = \phi(k) - \gamma \xi(\bar{\mathbf{x}}(k)) e(k+1) . \quad (59)$$

Noting that $\phi(k) := \theta^* - \delta(k)$, this adaptation law corresponds to the adaptation of $\theta(k)$ as seen in figure (2), given by

$$\theta(k+1) = \theta(k) + \gamma \xi(\bar{\mathbf{x}}(k)) e(k+1) . \quad (60)$$

Substituting the adaptation law of equation (59) into equation (58), we have

$$\begin{aligned} \Delta V(k) = e^2(k+1) + \frac{(\phi^T(k) - \gamma \xi^T(\bar{\mathbf{x}}(k)) e(k+1))(\phi(k) - \gamma \xi(\bar{\mathbf{x}}(k)) e(k+1))}{\gamma} \\ - e^2(k) - \frac{\phi^T(k)\phi(k)}{\gamma} . \end{aligned} \quad (61)$$

Since $\phi^T(k) \xi(\bar{\mathbf{x}}(k)) = \xi^T(\bar{\mathbf{x}}(k)) \phi(k)$, we have

$$\begin{aligned} \Delta V(k) = e^2(k+1) + \frac{\phi^T(k)\phi(k)}{\gamma} - \frac{2\gamma \phi^T(k) \xi(\bar{\mathbf{x}}(k)) e(k+1)}{\gamma} + \\ \frac{\gamma^2 \xi^T(\bar{\mathbf{x}}(k)) \xi(\bar{\mathbf{x}}(k)) e^2(k+1)}{\gamma} - e^2(k) - \frac{\phi^T(k)\phi(k)}{\gamma} \quad \text{and} \end{aligned} \quad (62)$$

$$\begin{aligned} \Delta V(k) = e^2(k+1) - e^2(k) \\ - 2\phi^T(k) \xi(\bar{\mathbf{x}}(k)) e(k+1) + \gamma \xi^T(\bar{\mathbf{x}}(k)) \xi(\bar{\mathbf{x}}(k)) e^2(k+1) . \end{aligned} \quad (63)$$

At this point, an intermediate Lyapunov analysis is performed to investigate the term $\phi(k)$. Consider a Lyapunov function

$$V_\phi(k) := \frac{\phi^T(k)\phi(k)}{\gamma} = \frac{1}{\gamma} \|\phi(k)\|_2^2. \quad (64)$$

The forward difference function, $\Delta V_\phi(k) := V_\phi(k+1) - V_\phi(k)$, becomes

$$\Delta V_\phi(k) = \frac{\phi^T(k+1)\phi(k+1)}{\gamma} - \frac{\phi^T(k)\phi(k)}{\gamma}. \quad (65)$$

As in the analysis for $\Delta V(k)$, we can arrive at

$$\begin{aligned} \Delta V_\phi(k) &= \frac{\phi^T(k)\phi(k)}{\gamma} - \frac{2\gamma\phi^T(k)\xi(\bar{\mathbf{x}}(k))e(k+1)}{\gamma} + \\ &\quad \frac{\gamma^2\xi^T(\bar{\mathbf{x}}(k))\xi(\bar{\mathbf{x}}(k))e^2(k+1)}{\gamma} - \frac{\phi^T(k)\phi(k)}{\gamma} \end{aligned} \quad (66)$$

and

$$\Delta V_\phi(k) = -2\phi^T(k)\xi(\bar{\mathbf{x}}(k))e(k+1) + \gamma\xi^T(\bar{\mathbf{x}}(k))\xi(\bar{\mathbf{x}}(k))e^2(k+1). \quad (67)$$

It is assumed that we are achieving $\|\mathbf{x}(t)\|_2 < M_x$ for $\{t \mid t_s k \leq t < t_s(k+1)\}$. If $\|\dot{\mathbf{x}}(t)\|_2 = M_x$ for any $\{t \mid t_s k \leq t < t_s(k+1)\}$ then $\delta_s(\mathbf{x}(t)) \neq 0$ for some $\{t \mid t_s k \leq t < t_s(k+1)\}$ and adaptation is turned off at this instance, k . Looking at the second term of equation (67), $-2\phi^T(k)\xi(\bar{\mathbf{x}}(k))e(k+1)$ and noting that adaptation only occurs when $|e(k+1)| > e^L$, the goal is to show that $2\phi^T(k)\xi(\bar{\mathbf{x}}(k))e(k+1)$ is always positive. Knowing $\phi(k) := \theta^* - \delta(k)$, we have

$$2\phi^T(k)\xi(\bar{\mathbf{x}}(k))e(k+1) = 2e(k+1) \sum_{i=1}^{n_r} [(\theta_i^* - \theta_i(k))\xi_i(\bar{\mathbf{x}}(k))]. \quad (68)$$

Suppose we have $e(k+1) > e_L$ or, in other words, $y_m(k+1) > y_p(k+1)$. Due to the relationship between δ_{j_b} and y_p , (which represents the yaw rate of the plant since $c = [0, 0, 0, 1]$), $e(k+1) > e_L$ implies that the actual feedback control term from the FLC, $\bar{\delta}_{j_b}(k)$, was less than the control needed to achieve $y_p(k)$. Thus, we have

$$\bar{\delta}_{j_b}(k) = \sum_{i=1}^{n_r} \theta_i(k)\xi_i(\bar{\mathbf{x}}(k)) < \sum_{i=1}^{n_r} \theta_i^*(k)\xi_i(\bar{\mathbf{x}}(k)), \quad (69)$$

from which we can deduce that

$$\phi^T(k)\xi(\bar{\mathbf{x}}(k)) = \sum_{i=1}^{n_r} \theta_i^*(k)\xi_i(\bar{\mathbf{x}}(k)) - \sum_{i=1}^{n_r} \theta_i(k)\xi_i(\bar{\mathbf{x}}(k)) > 0 . \quad (70)$$

Thus, we have

$$2\phi^T(k)\xi(\bar{\mathbf{x}}(k))e(k+1) > 0 . \quad (71)$$

If we suppose $e(k+1) < -e_L$, we can similarly deduce that

$$\phi^T(k)\xi(\bar{\mathbf{x}}(k)) < 0 . \quad (72)$$

Thus, for every $|e(k+1)| > e_L$, we have

$$2\phi^T(k)\xi(\bar{\mathbf{x}}(k))e(k+1) > 0 . \quad (73)$$

Returning to forward difference function, $\Delta V_\phi(k)$ of equation (67), we can establish that $\Delta V_\phi(k) < 0$ when

$$\gamma \xi^T(\bar{\mathbf{x}}(k))\xi(\bar{\mathbf{x}}(k))e^2(k+1) < 2\phi^T(k)\xi(\bar{\mathbf{x}}(k))e(k+1) \quad (74)$$

or recalling that $\xi^T(\bar{\mathbf{x}}(k))\xi(\bar{\mathbf{x}}(k)) \leq 1$ from equation (8)

$$\gamma < \frac{2|\phi^T(k)\xi(\bar{\mathbf{x}}(k))|}{|e(k+1)|} . \quad (75)$$

Noting that adaptation only occurs when $|e(k+1)| > e_L$, we can recall equation (56) to establish the inequality

$$|\phi^T(k)\xi(\bar{\mathbf{x}}(k))| \geq \frac{|e(k+1)|}{\bar{b}_4^U} - w^U, \quad (76)$$

where \bar{b}_4^U is defined such that $\bar{b}_4^U \geq \bar{b}_4$ over the range of vehicle parameters and road surface conditions and w^U is defined in equation (48).

Thus, equation (75) is satisfied if

$$\gamma < \frac{2\left(\frac{e_L}{\bar{b}_4^U} - w^U\right)}{|e(k+1)|}, \quad (77)$$

where $\frac{e_L}{\bar{b}_4^U} - w^U > 0$ as will be explained further in the analysis.

This condition states that during adaptation (which only occurs when $|e(k+1)| > e_L$) the term $\|\phi(k)\|_2$ will decrease.

Returning to the Lyapunov function $V(k)$ of equation (57), and its forward difference function $\Delta V(k)$, last modified in equation (63), with the condition on γ from equation (77), $\Delta V(k)$ is bounded by

$$\Delta V(k) \leq e^2(k+1) - e^2(k). \quad (78)$$

Now, assuming we achieve $\|\mathbf{x}(t)\|_2 < M_x$ for $\{t \mid t_s k \leq t < t_s(k+1)\}$, we substitute the expression for $e(k+1)$ from equation (56) to get

$$\Delta V(k) \leq \left(\bar{b}_4 \left(\phi^T(k) \xi(\bar{\mathbf{x}}(k)) - w(k) \right) \right)^2 - e^2(k) \quad (79)$$

and with the definitions of w^U and \bar{b}_4^U ,

$$\Delta V(k) \leq \left(\bar{b}_4^U \left(\left| \phi^T(k) \xi(\bar{\mathbf{x}}(k)) \right| + w^U \right) \right)^2 - e^2(k) \quad (80)$$

Furthermore, since $\left| \phi^T(k) \xi(\bar{\mathbf{x}}(k)) \right| \leq \|\phi(k)\|_2 \|\xi(\bar{\mathbf{x}}(k))\|_2$ and $\|\xi(\bar{\mathbf{x}}(k))\|_2 \leq 1$ from equation (8) we have

$$\Delta V(k) \leq \left(\bar{b}_4^U \left(\|\phi(k)\|_2 + w^U \right) \right)^2 - e^2(k) . \quad (81)$$

It can be concluded that $\Delta V(k) \leq 0$ will occur when

$$e^2(k) \geq \left(\bar{b}_4^U \left(\|\phi(k)\|_2 + w^U \right) \right)^2 \quad (82)$$

or

$$|e(k)| \geq \bar{b}_4^U \|\phi(k)\|_2 + \bar{b}_4^U w^U . \quad (83)$$

Figure 3 can be supplemented by adding the line $e(k) = \bar{b}_4^U \|\phi(k)\|_2 + \bar{b}_4^U w^U$, to obtain figure 4. It can be seen here that e_L must be chosen such that $e_L \geq \bar{b}_4^U w^U$, because the resolution of the FLC can not guarantee that $|e(k)| < \bar{b}_4^U w^U$ can be achieved.

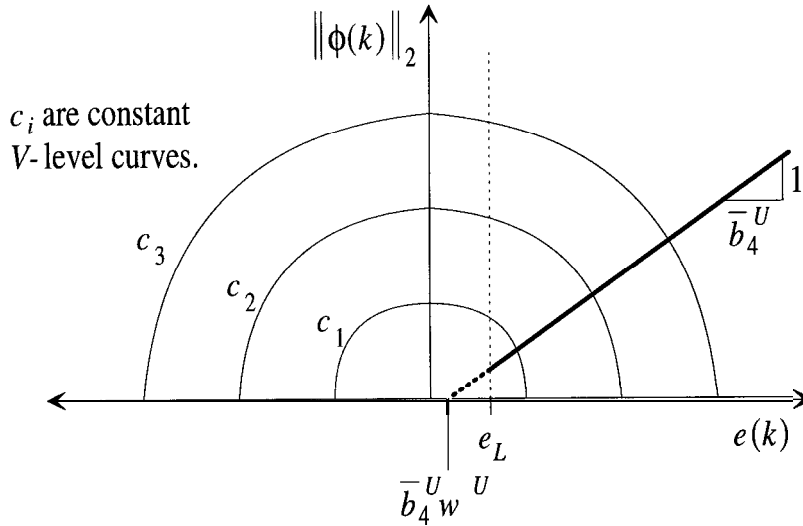


Figure 4: V-level Curves; Signal Flow

Arguments will be presented for the case when $e(k) > 0$, although symmetric arguments can be made for $e(k) < 0$. Suppose that at some instance $e(k) > e_L$. The error is small, as desired, but may increase as the control system propagates. However, since adaptation does *not* occur when $|e(k)| \leq e_L$, the term $\|\phi(k)\|_2$ does not change.

Suppose that $e(k)$ *does* increase such that at some instance $e(k) > e_L$, so adaptation *does* occur. Satisfying the constraint on the learning rate, γ , in equation (77), $\|\phi(k)\|_2$ will decrease. Although $e(k)$ may decrease as desired, this Lyapunov analysis provides only a sufficient condition that $\Delta V(k) \leq 0$ if $e(k)$ goes beyond the line $e(k) = \bar{b}_4^U \|\phi(k)\|_2 + \bar{b}_4^U w^U$. However, if $e(k)$ does go beyond the line $e(k) = \bar{b}_4^U \|\phi(k)\|_2 + \bar{b}_4^U w^U$, the propagation of $e(k)$, given by equation (56), shows that $e(k)$ will be pushed back to the line or to the left of the line, $e(k) = \bar{b}_4^U \|\phi(k)\|_2 + \bar{b}_4^U w^U$. This fact coupled with the fact that $\|\phi(k)\|_2$ is indeed decreasing at every propagation step, shows that in two propagation steps of $e(k)$, $e(k)$ will also decrease. This decrease in $e(k)$ will occur until $|e(k)| \leq e_L$. Thus, figure 5 shows the boundedness of $e(k)$ and $\|\phi(k)\|_2$ denoted by the blackened region when the system is initialized at either points 1 or 2, and furthermore, $|e(k)|$ approaches e_L . In

addition, given sufficient excitation of the system, $\|\phi(k)\|_2$ will approach to the point where the lines $e(k) = e_L$ and $e(k) = \bar{b}_4^U \|\phi(k)\|_2 + \bar{b}_4^U w^U$ intersect, which is at $\|\phi(k)\|_2 = \frac{e_L}{\bar{b}_4^U} - w^U$.

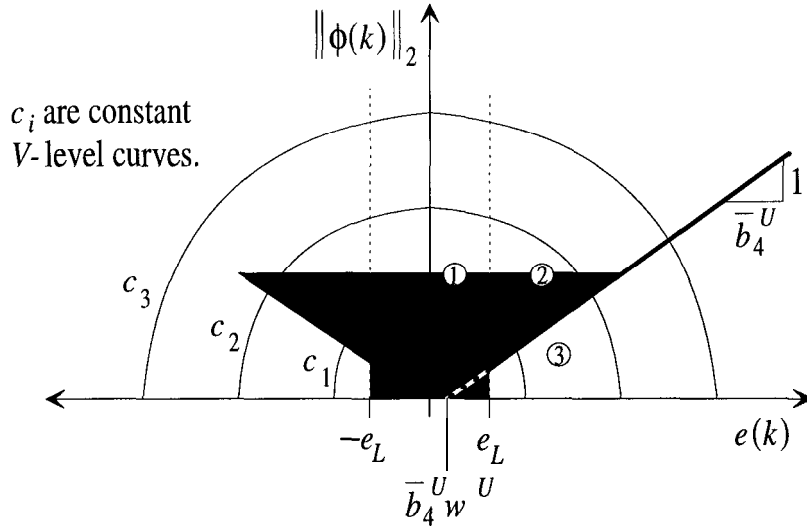


Figure 5: Error bounds

Note that if the system is at some instance at point 3 on figure 5, the propagation of $e(k+1)$ as given by equation (56), will push the point to the left of the line, $e(k) = \bar{b}_4^U \|\phi(k)\|_2 + \bar{b}_4^U w^U$, and the above arguments will apply.

A remark needs to be made about the assumption that $\|\mathbf{x}(t)\|_2 < M_x$ for $\{t \mid t_s k \leq t < t_s(k+1)\}$. If $\|\mathbf{x}(t)\|_2 = M_x$ for any $\{t \mid t_s k \leq t < t_s(k+1)\}$ then $\delta_s(\mathbf{x}(t)) \neq 0$ for some $\{t \mid t_s k \leq t < t_s(k+1)\}$. At this instance k , adaptation is turned off, since there is now way to guarantee that $\|\phi(k)\|_2$ will decrease at that instance. However, assuming that $\|\mathbf{x}(t)\|_2 = M_x$ only on some time intervals $\{t \mid t_s k \leq t < t_s(k+1)\}$, then adaptation *will* occur on the other intervals. Thus, the arguments above regarding propagation of $\phi(k)$ and $e(k)$ continue to hold. There appears to be a design tradeoff which depends on the choice of M_x . If M_x is chosen to be larger, then $\|\mathbf{x}(t)\|_2 = M_x$ will only rarely occur, if at all. However, the region where the states are bounded, $\|\mathbf{x}(t)\|_2 \leq M_x$, will also be larger. Thus, it is more difficult for the FLC to approximate the optimal control, $\delta''(k)$, and the adaptation will take longer.

5 Application to FLC Vehicle Guidance

In this section the MRAFLC is formulated specifically for the feedback and preview rule bases for lateral control of a vehicle. The adaptation for the feedback and preview rule bases are not implemented simultaneously. The initial rule bases before adaptation are the rule bases resulting from the manually tuned rule bases [2].

5.1 Feedback Rule Base

Figure 6 shows the block diagram for the feedback rule base adaptation scheme.

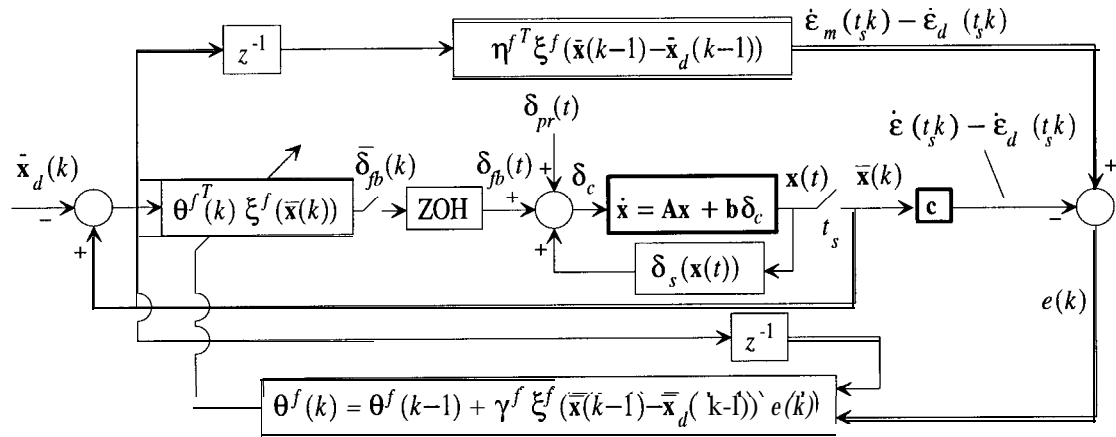


Figure 6: Feedback MRAFLC Block Diagram

The feedback rule base investigated using this adaptation scheme uses full-state feedback, equation (2), which has the following input variables:

$$T(k) := \begin{bmatrix} \bar{x}_1(k) \\ \bar{x}_2(k) \\ \bar{x}_3(k) \\ \bar{x}_4(k) \end{bmatrix} = \begin{bmatrix} y_r(t_s k) & \mathbf{1} \\ \dot{y}_r(t_s k) \\ \epsilon(t_s k) - \epsilon_d(t_s k) \\ \dot{\epsilon}(t_s k) - \dot{\epsilon}_d(t_s k) \end{bmatrix}. \quad (84)$$

The feedback fuzzy rule base infers a feedback front wheel steering angle command given by

$$\bar{\delta}_{fb}(k) = \theta^{fT}(k) \xi^f(\bar{\mathbf{x}}(k)). \quad (85)$$

The vector of fuzzy basis functions is given by

$$\xi^f(\bar{\mathbf{x}}(k)) := \{\xi_s^f(\bar{\mathbf{x}}(k))\}_{s=1}^{n_{fb}}, \quad (86)$$

where n_{fb} is the total number of feedback fuzzy rules in the rule base and $\xi_s^f(\bar{\mathbf{x}}(k))$ are defined by

$$\xi_s^f(\bar{\mathbf{x}}(k)) := \frac{\prod_{i=1}^4 \mu_i^s(\bar{x}_i(k))}{\sum_{l=1}^{n_{fb}} \left(\prod_{i=1}^4 \mu_i^l(\bar{x}_i(k)) \right)} \quad \text{for } s = 1, 2, \dots, n_{fb}. \quad (87)$$

The term $\mu_i^s(\bar{x}_i(k))$ is the membership function for the i -th input variable ($i = 1, 2, 3, 4$), and for the s -th rule ($s = 1, \dots, n_{fb}$). The membership functions for this adaptation investigation are precisely defined in appendix A.

The adaptable consequent singleton parameters for the feedback rule base are given by

$$\theta^f(k) := \{\theta_s^f(k)\}_{s=1}^{n_{fb}}, \quad (88)$$

The MRAFLC for the feedback rule base is designed to follow the relative yaw rate, $\dot{\bar{e}}_m(t_s k) - \dot{\bar{e}}_d(t_s k)$, (i.e., the actual yaw rate with respect to a desired yaw rate set by the road curvature, $\dot{\bar{e}}_d = v_x / \rho$). The model is given by the following fuzzy system:

$$\dot{\bar{e}}_m(t_s k) - \dot{\bar{e}}_d(t_s k) = \eta^{fT} \xi^f(\bar{\mathbf{x}}(k-1) - \bar{\mathbf{x}}_d(k-1)) . \quad (89)$$

where the consequent singletons of the model fuzzy system are given by

$$\eta^f := \{\eta_s^f\}_{s=1}^{n_p} . \quad (90)$$

Recalling equation (59) and $\phi(k) := \theta^* - \theta(k)$ the adaptation law for the feedback rule base is given by

$$\theta^f(k) = \theta^f(k-1) + \gamma^f \xi^f(\bar{\mathbf{x}}(k-1) - \bar{\mathbf{x}}_d(k-1)) e(k) , \quad (91)$$

where the model reference error term is given by

$$e(k) := (\dot{\bar{e}}_m(t_s k) - \dot{\bar{e}}_d(t_s k)) - (\dot{\bar{e}}(t_s k) - \dot{\bar{e}}_d(t_s k)) = \dot{\bar{e}}_m(t_s k) - \dot{\bar{e}}(t_s k) . \quad (92)$$

5.2 Preview Rule Base

The formulation for the adaptation of the preview rule base is similar to that of the feedback rule base. The initial preview rule base before adaptation is the preview rule base resulting from the manually tuned preview rule base of [2]. Figure 7 shows the block diagram for the preview rule base adaptation scheme.

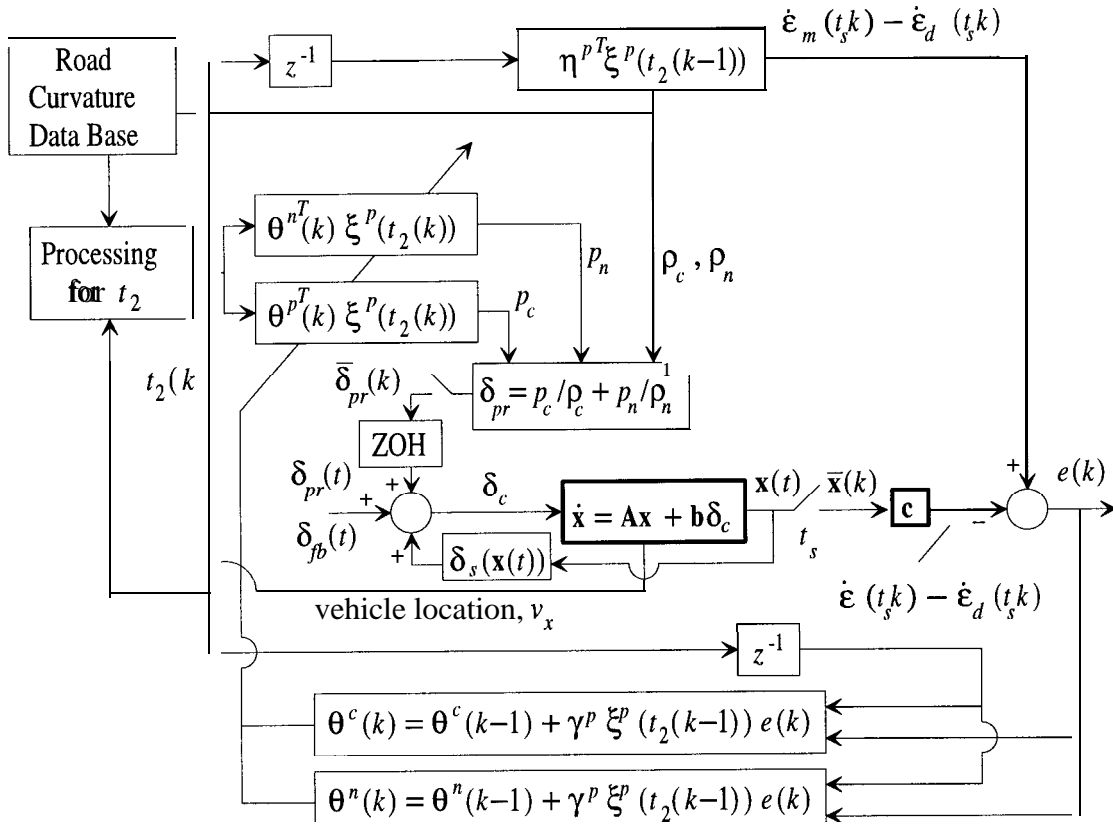


Figure 7: Preview MRAFLC Block Diagram

The preview rule base has only one input variable, the time for the vehicle to reach the next curve transition, t_2 , defined as:

$$t_2(k) := \frac{\text{curve transition location} - \text{vehicle location}}{v_x}, \quad (93)$$

where v_x is the longitudinal velocity.

The preview fuzzy rule base infers the parameters p_c and p_n , which are used in an expression to calculate a preview front wheel steering angle command. The fuzzy systems which determine p_c and p_n are given by

$$p_c(k) = \theta^{cT}(k) \xi^p(t_2(k)) \quad \text{and} \quad (94)$$

$$p_n(k) = \theta^{nT}(k) \xi^p(t_2(k)). \quad (95)$$

The expression to calculate a preview front wheel steering angle command, $\bar{\delta}_{pr}$, is given by

$$\bar{\delta}_{pr}(k) = \frac{p_c(k)}{\rho_c(k)} + \frac{p_n(k)}{\rho_n(k)}. \quad (96)$$

The vector of fuzzy basis functions are given by

$$\xi^p(t_2(k)) := \left\{ \xi_s^p(t_2(k)) \right\}_{s=1}^{n_{pr}}, \quad (97)$$

where n_{pr} is the total number of preview fuzzy rules in the rule base, and $\xi_s^p(t_2(k))$ is defined by

$$\xi_s^p(t_2(k)) := \frac{\mu^s(t_2(k))}{\sum_{l=1}^{n_{pr}} \mu^l(t_2(k))} \quad \text{for } s = 1, 2, \dots, n_{pr}. \quad (98)$$

The term $\mu^s(t_2(k))$ is the membership function for the input variable, t_2 , for the s -th rule ($s = 1, \dots, n_{pr}$). The membership functions for this adaptation investigation are precisely defined in appendix A.

The adaptable consequent singleton parameters for the preview rule base are given by

$$\theta^c(k) := \{\theta_s^c(k)\}_{s=1}^{n_{pr}} \text{ and} \quad (99)$$

$$\theta^n(k) := \{\theta_s^n(k)\}_{s=1}^{n_{pr}} . \quad (100)$$

The MRAFLC for the preview rule base is designed to follow the relative yaw rate, $\dot{\epsilon}_m(t_s k) - \dot{\epsilon}_d(t_s k)$. The model is given by the following fuzzy system:

$$\dot{\epsilon}_m(t_s k) - \dot{\epsilon}_d(t_s k) = \eta^{pT} \xi^p(t_2(k-1)) . \quad (101)$$

where the consequent singletons of the model fuzzy system are given by

$$\eta^f := \{\eta_s^f\}_{s=1}^{n_{fp}} . \quad (102)$$

The adaptation law for the preview rule base is given by

$$\theta^c(k) = \theta^c(k-1) + \gamma^p \xi^p(t_2(k-1)) e(k) \text{ and} \quad (103)$$

$$\theta^n(k) = \theta^n(k-1) + \gamma^p \xi^p(t_2(k-1)) e(k) , \quad (104)$$

where the model reference error term is given by

$$e(k) := (\dot{\epsilon}_m(t_s k) - \dot{\epsilon}_d(t_s k)) - (\dot{\epsilon}(t_s k) - \dot{\epsilon}_d(t_s k)) = \dot{\epsilon}_m(t_s k) - \dot{\epsilon}(t_s k) . \quad (105)$$

6 MRAFLC Simulation Results for Vehicle Guidance

In this section the simulation results of the FLC algorithms for lateral vehicle guidance tuned by the model reference adaptive method (MRAFLC) are presented. The

first section shows the results of the *feedback* rule base, and the second section shows the results of the *preview* rule base.

6.1 Feedback Rule Base

The simulations for the feedback controllers are performed without using any preview information. The model reference adaptive fuzzy logic controllers (MRAFLC) are tuned for the feedback rule base during simulations where the vehicle starts at a 0.1 meter lateral error, and its lateral motion is regulated on a straight roadway. The MRAFLC is being adapted continuously throughout the simulations at time steps of 0.01 seconds with an adaptation rate, γ , equal to 0.6, which was chosen based on performance of the simulations, and will be shown in the discussion of the simulation results to satisfy the proper conditions. The specified limit of the output error term ($e = \dot{\hat{e}}_m - \dot{\hat{e}}$, i.e., actual relative to modeled yaw rate), e_L , is specified as 0.01 rad/sec (see section 4). The typical yaw rate magnitudes range up to 0.04 rad/sec. The term e_L can not be made too small as that would place an overly restrictive constraint on the adaptation rate γ , which as seen in section 4, must satisfy

$$\gamma < \frac{2 \left(\frac{e_L}{b_4^U} - w^U \right)}{|e(k)|} \quad (106)$$

The term \bar{b}_4^U , defined in the previous sections, (which is the upper bound of the 4-th element of the 4×1 column vector, $\bar{\mathbf{b}}$, discussed in section 2), is determined to be $\bar{b}_4^U = 0.4 \text{ sec.}^{-1}$ by using extreme values of vehicle parameters and road surface conditions. As defined in section 2, w^U is defined such that for the input vector $\bar{\mathbf{x}}(k) = [y_r(t_s k), \dot{y}_r(t_s k), \varepsilon(t_s k) - \varepsilon_d(t_s k), \dot{\varepsilon}(t_s k) - \dot{\varepsilon}_d(t_s k)]^T$, with $t_s = 0.01 \text{ second}$,

$$\sup_{\bar{\mathbf{x}} \mid \|\bar{\mathbf{x}}\|_2 \leq M_x} \left| \delta^* - \theta^{*T} \xi(\bar{\mathbf{x}}(k)) \right| \leq w^U, \quad (107)$$

where $\delta^* = \frac{\eta^T \xi(\bar{\mathbf{x}}(k)) - \sum_{i=1}^4 \bar{A}_{4i} \bar{x}_i}{\bar{b}_4}$, of which θ^* , η , $\xi(\bar{\mathbf{x}}(k))$, \bar{A}_{4i} , and \bar{b}_4 are precisely defined in section 2. Since the term θ^* is not available, the term, w^U , is estimated numerically by

$$w^U = \max_{\bar{\mathbf{x}}_j \mid \|\bar{\mathbf{x}}_j\|_2 \leq M_x} \left| \delta^* - \theta(k)^T \xi(\bar{\mathbf{x}}_j(k)) \right|, \quad (108)$$

where the calculation of $\left| \delta^* - \theta(k)^T \xi(\bar{\mathbf{x}}_j(k)) \right|$ is performed after adaptation at discrete points, $\bar{\mathbf{x}}_j$, where control action occurred. In the following simulations, a numerical calculation of w^U will be obtained using the term $e(k)$ instead of θ^* . Since $e(k)$ approaches θ^* during adaptation, the estimation of w^U which satisfy the definition of w^U is improved as the adaptation progresses.

With specified or calculated values for e_L , \bar{b}_4^U , and w^U , along with the largest value of $|e(k)|$ taken as 0.035 rad/sec in the simulations, the choice of γ can be justified in the following simulations using equation (106). It can be noted in the simulation discussions that the results consistently show that $w^U \ll e^L / \bar{b}_4^U$ by a magnitude of 10, implying good resolution of the FLC. The term M_x is chosen large enough such that for the following simulations $\|\mathbf{x}(t)\|_2 < M_x$ is satisfied. This results in $\delta_x(t) \equiv 0$ for all t , providing a true test of the quality of the fuzzy reference model and the validity of the convergence properties of the MRAFLC discussed in the previous sections.

The effectiveness of this adaptation scheme to properly tune the controller is best demonstrated considering the nominal speed of $v_x = 20.0 \text{ m/s}$, where the goal is to fine

tune the controller. The effectiveness of the MRAFLC in addressing changing operating conditions is shown by simulations of an increased vehicle speed to $v_x = 30.0$ m/s, and of a slippery road condition at $v_x = 20.0$ m/s.

Figure 8 shows the simulation results for a “nominal” system, using the feedback rule base of the FLC which uses the fuzzy controller with \mathbf{x}_1 as its input. The longitudinal velocity, v_x , equals 20.0 m/s, and the cornering stiffness for all four tires, C_s , equals 42,000 N. The simulation results compare the responses of the original fuzzy logic controller before adaptation, with the initial response of the adaptation method of the MRAFLC on the feedback rule base. Furthermore, after the vehicle was simulated at different initial conditions, allowing for approximately 20 seconds of adaptation, the resulting response of the adapted MRAFLC is shown along with the FSLQ controller for additional comparisons. The purpose of showing the response after 20 seconds of adaptation is to demonstrate the capability of the MRAFLC to tune a roughly designed FLC such that the adapted FLC improves its performance.

After the 20 seconds of adaptation, w^U was estimated to be $w^U \approx 0.002$ rad., resulting in a requirement of $\gamma < 1.4$. Thus, the choice of $\gamma = 0.6$ is justified. The worst error measurement after the 20 seconds of adaptation was $|e| \approx 0.006$ rad / sec., which satisfies the specification of $e_L = 0.01$ rad/sec. Observing the steering angle command response, the adaptation method is seen to reduce the oscillations of δ_c , which results in smoother ride comfort as seen in the yaw rate and lateral acceleration responses. Also, observing the tracking error response curves, the over damping characteristics of the original rule base are eliminated by the adaptation method.

Figure 9 shows the simulation results of the comparison between the actual yaw rate and the reference yaw rate generated from the model reference fuzzy system. From this figure, the estimate of the error measurement after the 20 seconds of adaptation can be observed to be $|e| \approx 0.006$ rad / sec.

FLC/No A d a p t i n g ; FLC/MRAFLC (initial) - - - ;
 FLC/MRAFLC (after adapting 20 sec.) ——— ; FSLQ - - -

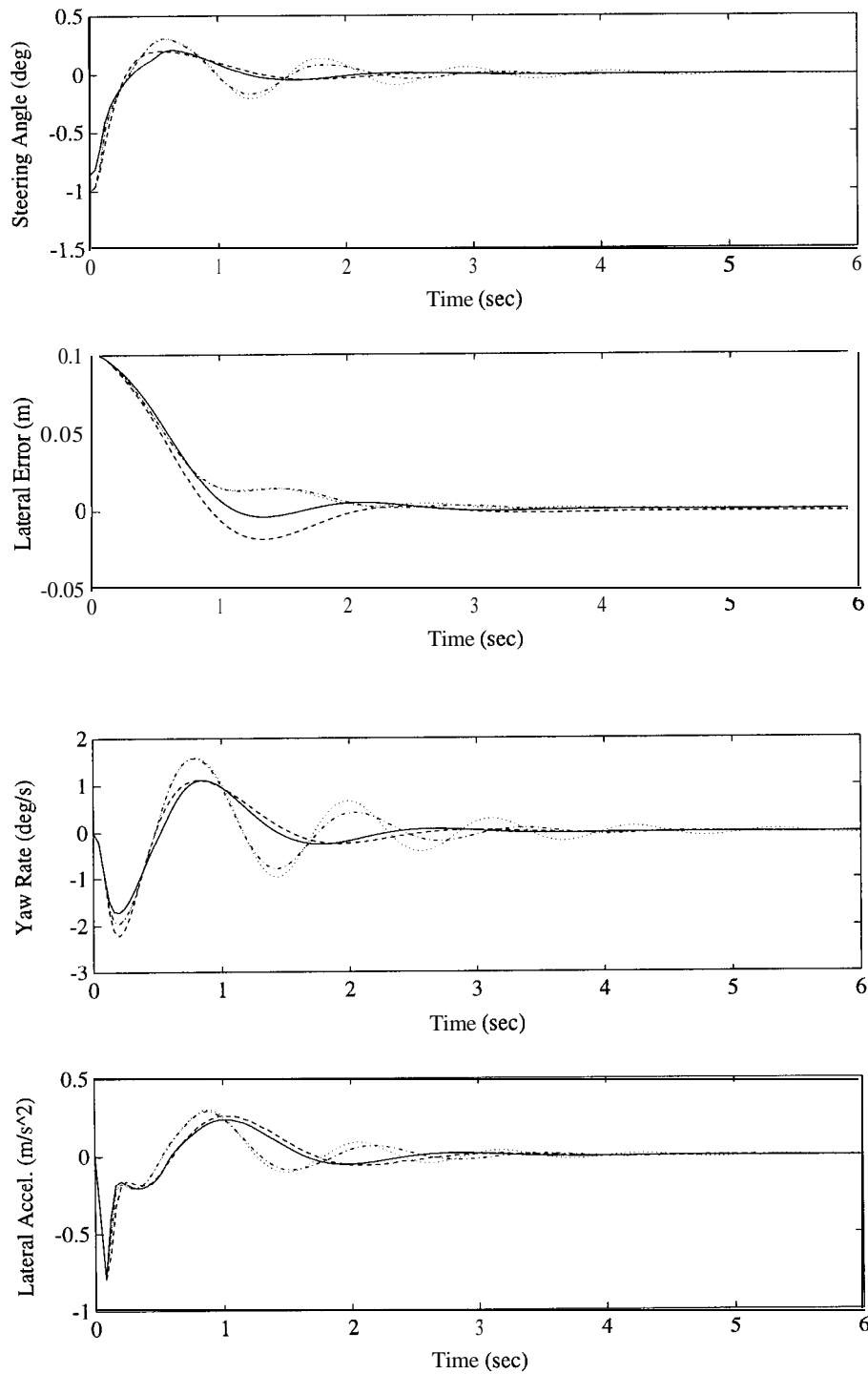


Figure 8: Closed-loop Simulation for FLC using x with and without adaptation by MRAFLC, and FSLQ (nominal conditions)

MRAFLC Reference - ; FLC(\mathbf{x}_1)/MRAFLC (after adapting 20 sec.) — ;

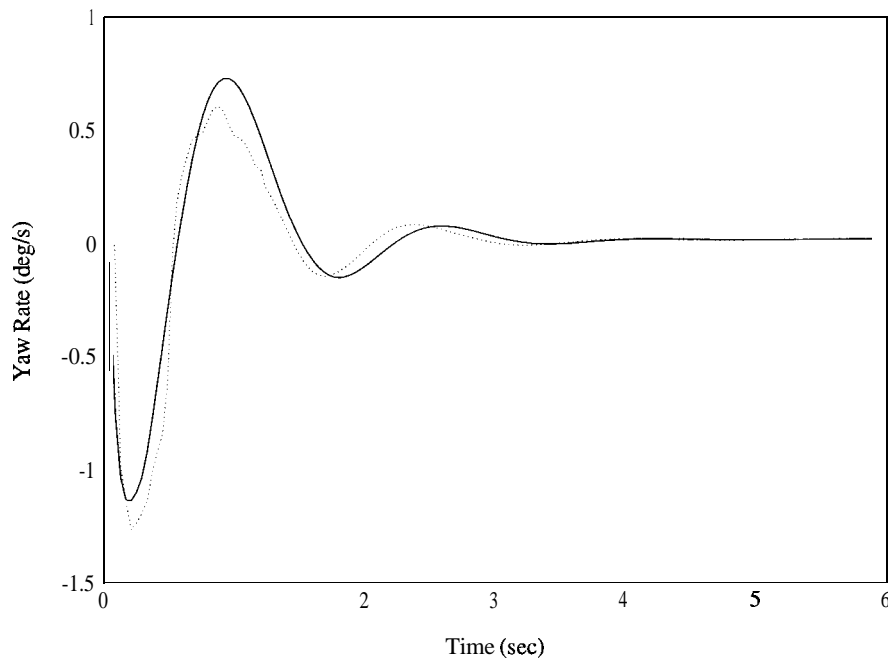


Figure 9: Actual Yaw Rate Compared to Model Reference Yaw Rate

Figure 11 shows the simulation results to show the effect of choosing γ to be too large. The original rule base is the same original rule base used for the adaptation of the “nominal” system in the previous simulation. The MRAFLC was tested by choosing γ to be 20, which violated the sufficient condition of $\gamma < 1.4$. Observing the steering angle command, the control system exhibits highly oscillatory, unstable behavior.

Figure 11 shows the simulation results for the vehicle traveling at a “high speed”. At the simulation time of $t = 0.5$ seconds, the longitudinal velocity of the vehicle is increased from $v_x = 20.0$ m/s to $v_x = 30.0$ m/s (with about a 1 second time lag). The original rule base is the same original rule base used for the adaptation of the “nominal” system. As can be seen by the dotted line, the original FLC design, designed for lower velocities, resulted in very large oscillations of δ_c , which in turn, resulted in very oscillatory behavior of the closed-loop system. Observing the steering angle command response, the adaptation method is seen to significantly reduce the oscillations of δ_c , resulting in smoother ride comfort as seen in the yaw rate and lateral acceleration

responses. Thus, it appeared that the adaptation required approximately 2 seconds to achieve a smooth steering angle command.

Figure 12 shows the simulation results for the vehicle traveling on a “slippery road”. At the simulation time of $t = 0.5$ seconds, the cornering stiffness is decreased from $C_s = 42,000$ N to $C_s = 24,000$ N. Again, the original rule base is the same original rule base used for the adaptation of the “nominal” system. Slippery road conditions caused the closed-loop response of the original rule base controller to have very large oscillations, as can be seen by the dotted line. Observing the steering angle command response, the adaptation method is seen to significantly reduce the oscillations of δ_c , resulting in smoother ride comfort as seen in the yaw rate and lateral acceleration responses, and improved tracking. Thus, it appeared that the adaptation required approximately 2 seconds to achieve a smooth steering angle command, after the vehicle encountered slippery road conditions.

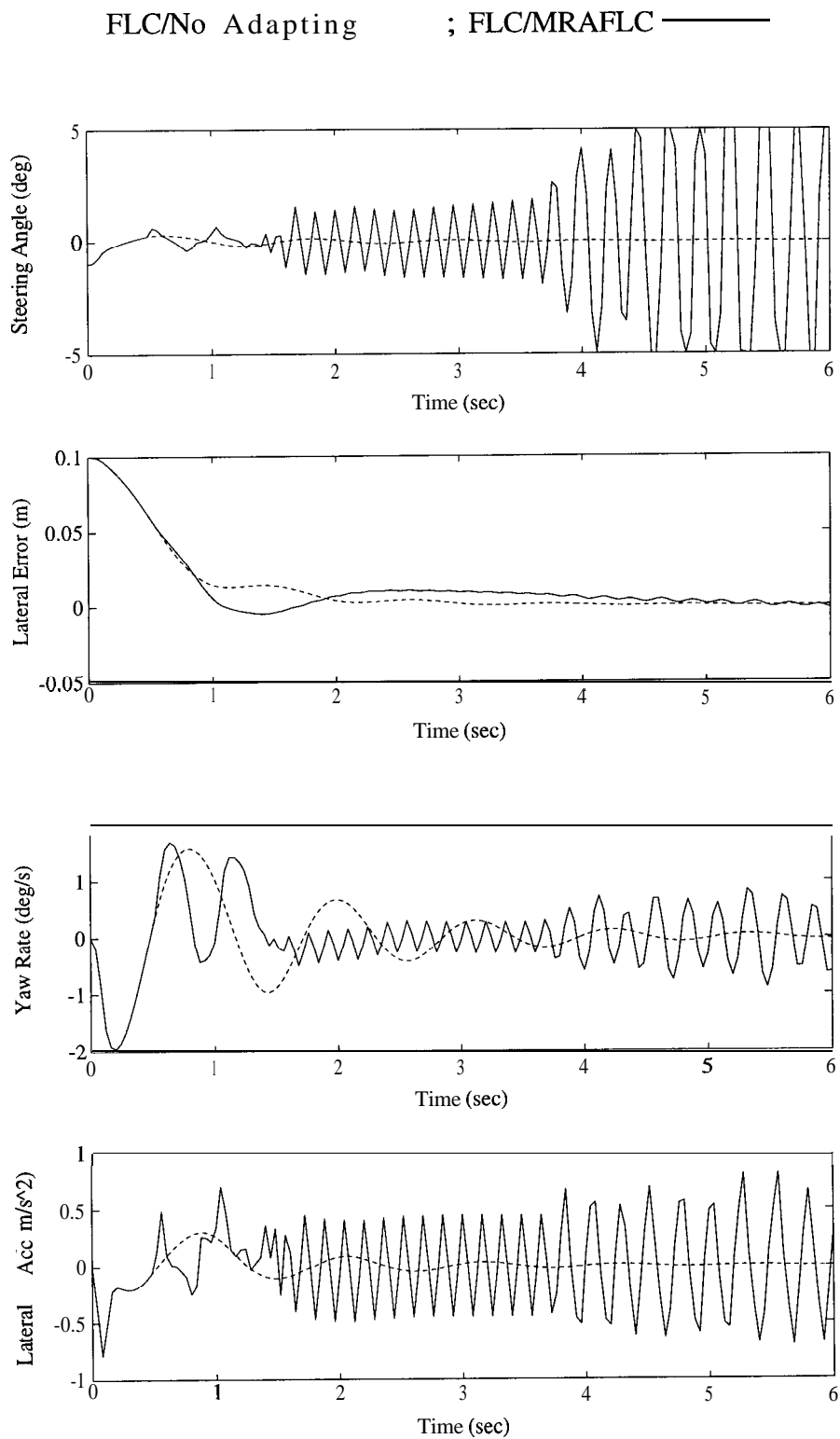


Figure 10: Closed-loop Simulation for FLC using x with and without adaptation by MRAFLC with large γ , exhibiting instability

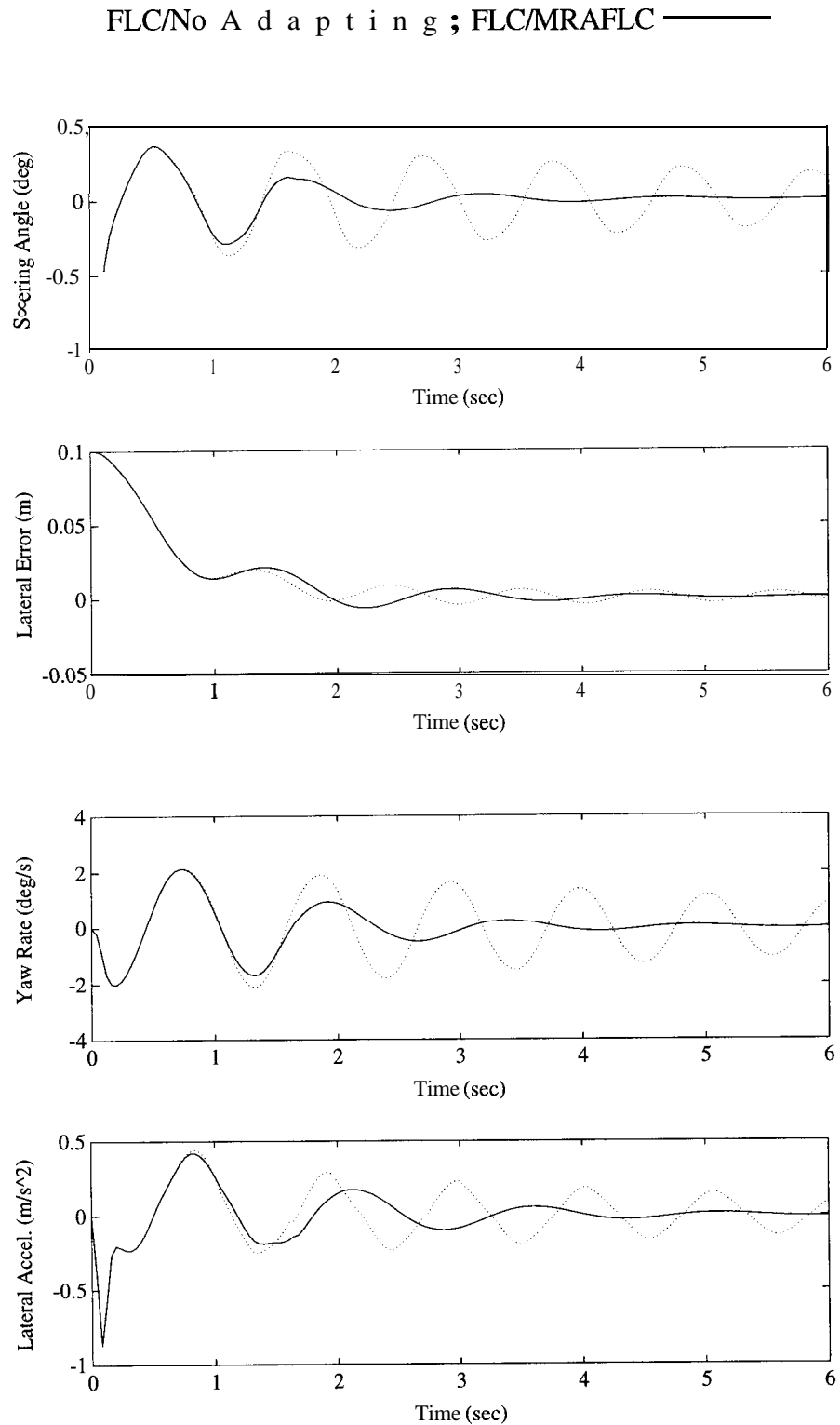


Figure 11: Closed-loop Simulation for FLC using x with and without adaptation by MRAFLC, (high speed)

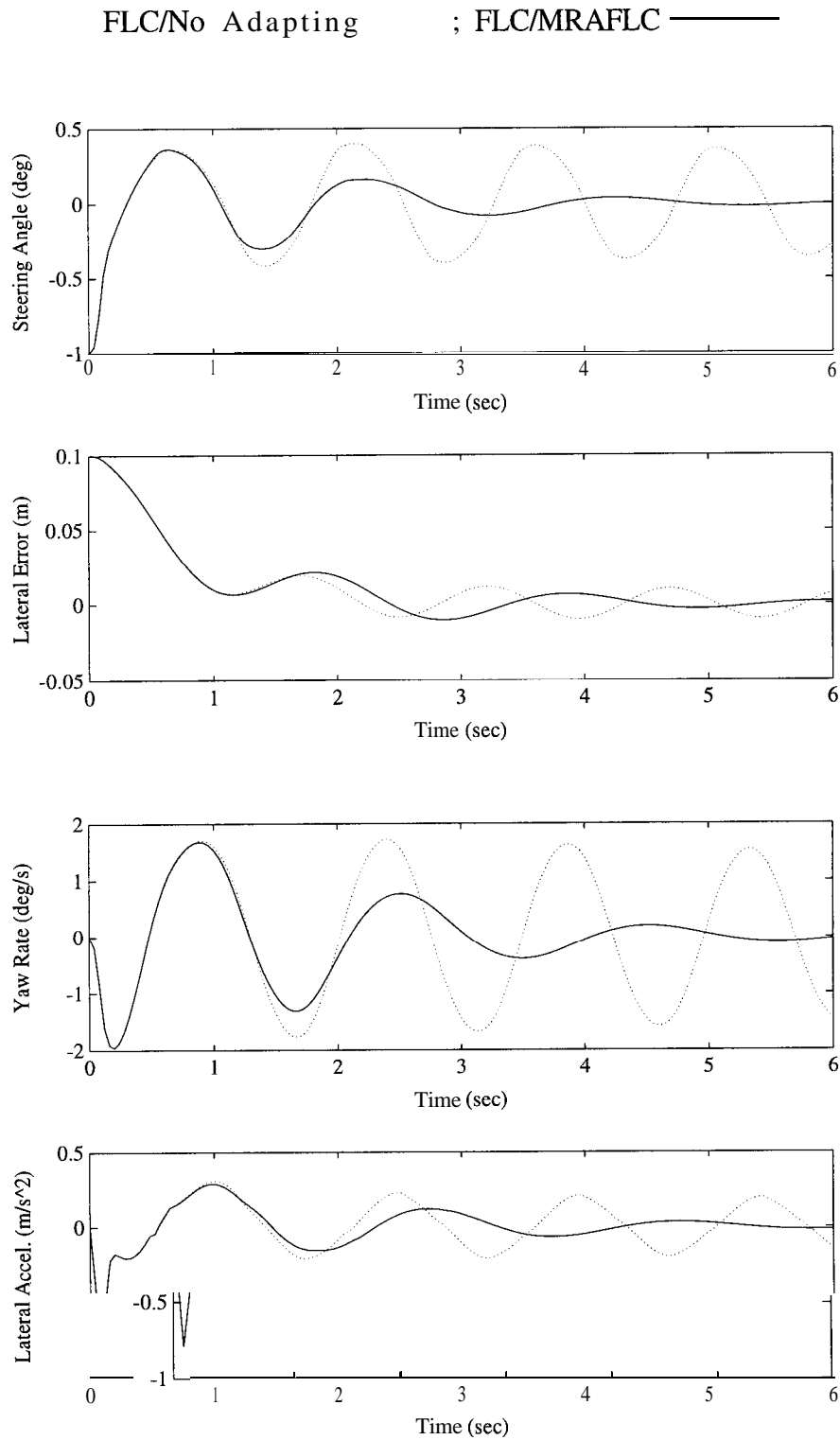


Figure 12: Closed-loop Simulation for FLC using x with and without adaptation by MRAFLC, (slippery road)

6.2 Preview Rule Base

In this section the preview controller using the MRAFLC is investigated. The simulations are performed using preview information regarding upcoming road curvature. The MRAFLC is tuned for the preview rule base during simulations where the vehicle starts at a 0.0 meter lateral error, and regulating its lateral motion on the curved track of figure 13. The feedback rule base of the FLC using the fuzzy controller with x as its input, was fixed during the preview adaptation. The MRAFLC is being adapted continuously throughout the simulation at time steps of 0.01 seconds with a adaptation rate, γ , equal to 0.6. This adaptation scheme is demonstrated considering the nominal speed of $v_x = 20.0$ m/s.

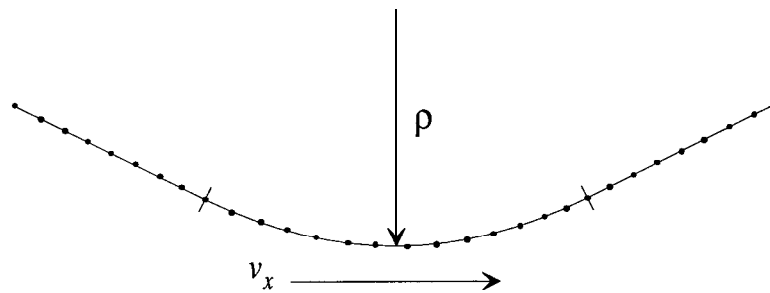


Figure 13: Simulation Test Track

Figure 14 shows the simulation results for a “nominal” system. The longitudinal velocity, v_x , equals 20.0 m/s, and the cornering stiffness for all four tires, C_s , equals 42,000 N. The simulation results compare the responses of the original fuzzy logic controller before adaptation, with the initial response of the adaptation method of the MRAFLC on the preview rule base. Furthermore, after the vehicle was simulated over five curved sections, which is 10 seconds of adaptation since there is a 1 second preview window for both the beginning and end of each curve, the resulting response of the adapted MRAFLC is shown along with the FSLQ controller for additional comparisons. The purpose of showing the response after 10 seconds of adaptation is to demonstrate the capability of the MRAFLC to tune a roughly designed preview FLC such that the adapted FLC improves its performance. Observing the lateral error response, the tracking performance is improved as the preview rule base is adapted. The overshoot at curve transitions is reduced and the average lateral error around the curved sections is reduced.

FLC/No Adapting ; FLC/MRAFLC (initial) - - - - ;
 FLC/MRAFLC (after adapting 5 sec.) ———— ; FSLQ - - - -

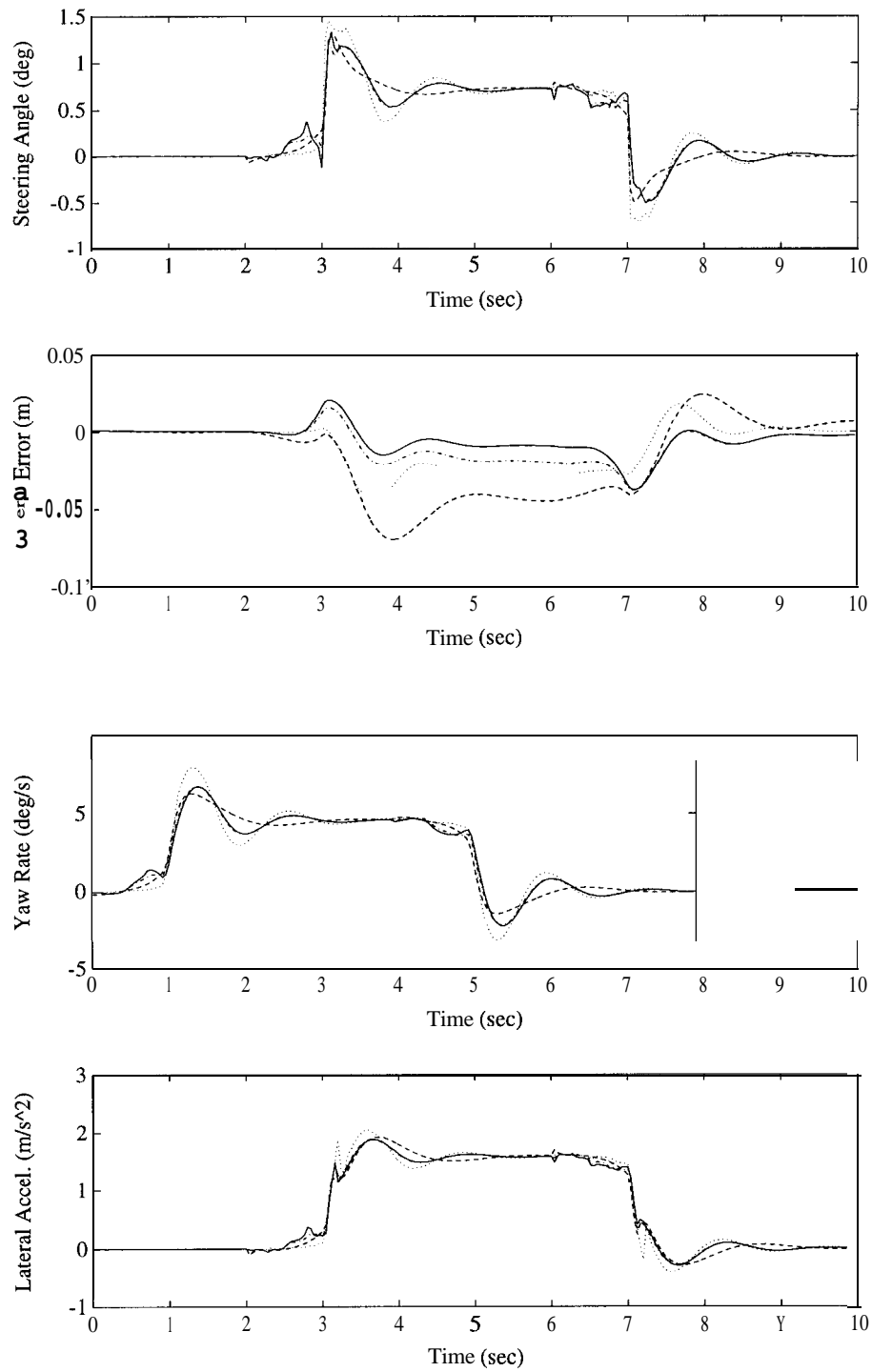


Figure 14: Closed-loop Simulation for FLC using x with and without adaptation by MRAFLC, and FSLQ/Prev. (nominal conditions)

7 Conclusion

An adaptive scheme of tuning the closed-loop control system was developed based on a model reference. The overall adaptive control system is called a model reference adaptive fuzzy logic controller (MRAFLC). The adaptation of the controller parameters by the MRAFLC is conducted on-line. The goal of this method is to adjust the parameters of the controller such that the output of the vehicle follows a desired output. The desired output is generated by a fuzzy system which has as its inputs, the states of the vehicle in the past, and as its system output, the desired output of the vehicle.

The simulation results showed that the adaptation law can shape the response of the closed-loop system to follow the response of a reference fuzzy system. A Lyapunov analysis was used to investigate the existence of a bound on the error between the desired and actual output of the closed-loop system. The results provided conditions on the adaptation law such that bounds on the output error could be achieved.

References

- [1] Astrom, K.J., Wittenmark, B., 1989. Adaptive Control, Reading, Massachusetts, Addison-Wesley.
- [2] Hessburg, T., Peng, H., Zhang, W.B., Arai, A., Tomizuka, M., February, 1994. "Experimental Results of Fuzzy Logic Control for Lateral Vehicle Guidance", Publication of PATH project, ITS, UC Berkeley, UCB-ITS-PRR-94-03.
- [3] Jang, R., 1992. "Self-Learning Fuzzy Controllers Based on Temporal Back Propagation", *IEEE Transactions on Neural Networks*, Vol. 3, No. 5, p. 714.
- [4] Karr, C., 1991. "Design of an Adaptive Fuzzy Logic Controller using a Genetic Algorithm", *Proc. of the Int'l Conference on Genetic Algorithms (ICGA'91)*, p. 450.
- [5] Kiszka, J., Gupta, M., Nikiforuk, P., 1985. "Energetic Stability of Fuzzy Dynamic Systems", *IEEE Trans. on Systems, Man, and Cybernetics*, Vol. SMC-15, No. 5, pp. 783-792.
- [6] Landau, I.D., Courtiol, B., 1974. "Design of Multivariable Adaptive Model Following Control Systems", *Automatica*, Vol. 10, pp. 483-494.
- [7] Langari, G., Tomizuka, M., December 1990. "Stability of Fuzzy Linguistic Control Systems", *Proc. of IEEE Conference on Decision and Control*, Hawaii.
- [8] Layne, J.R., Passino, K.M., December 1993. "Fuzzy Model Reference Learning Control for Cargo Ship Steering", *IEEE Control Systems Magazine*, 13(6), pp. 23-34.
- [9] Layne, J.R., Passino, K.M., Yurkovich, S., June 1993. "Fuzzy Learning Control for Antiskid Braking Systems", *IEEE Trans. on Control Systems Technology*, 1(2), pp. 122-129.
- [10] Narendra, K.S., Kudva, P., November 1974. "Stable Adaptive Schemes for System Identification and Control-Part I", *IEEE Trans. on Systems, Man, and Cybernetics*, Vol. SMC-4, No. 6, pp. 542-551.
- [11] Narendra, K.S., Kudva, P., November 1974. "Stable Adaptive Schemes for System Identification and Control-Part II", *IEEE Trans. on Systems, Man, and Cybernetics*, Vol. SMC4, No. 6, pp. 552-560.
- [12] Narendra, K.S., Lin, Y.H., July, 1991. "Stable Discrete Adaptive Control", *IEEE Trans. on Automatic Control*, Vol. AC-25, No. 3, June 1980, pp. 456-461.
- [13] Nomura, H., Hayashi, I., and Wakami, N., "A Self-tuning Method of Fuzzy Control by Descent Method", *4th IFSA Congress*, Vol. Engineering, p. 155.
- [14] Nomura, H., Hayashi, I., and Wakami, N., 1992. "A Self-tuning Method of Fuzzy Reasoning by Genetic Algorithm", *Proc. of the Int'l Fuzzy Systems and Intelligent Control Conference (IFSICC'92)*, Louisville, KY, p. 236.
- [15] Peng, H., Tomizuka, M., July 1990. "Lateral Control of Front-Wheel-Steering Rubber-Tire Vehicles", Publication of PATH project, ITS, UC Berkeley, UCB-ITS-PRR-90-5.
- [16] Procyk, T.J., Mamdani, E.H., 1979. "A Linguistic Self-Organizing Process Controller", *Automatica*, Vol. 15, pp. 15-30.
- [17] Shao, S., 1988. "Fuzzy Self-Organizing Controller and its Application for Dynamic Processes", *Fuzzy Sets and Systems*, Vol. 26, pp. 151-164.
- [18] Takagi, H., Hayashi, I., 1991. "INN-driven Fuzzy Reasoning", *Int'l. Journal of Approximate Reasoning* (Special Issue of IIZUKA '88), Vol. 5, NO. 3, p. 191.
- [19] Wang, L.X., 1992. "Fuzzy Systems are Universal Approximators", *Proc. of IEEE Int'l. Conference on Fuzzy Systems*, San Diego, CA, pp. 1163-1169.
- [20] Wang, L.X., 1992. Mendel, J.M., "Fuzzy Basis Functions, Universal Approximation, and Orthogonal Least Squares Learning", *IEEE Trans. on Neural Networks*, pp. 807-814.
- [21] Wang, L.X., 1993. "Stable Adaptive Fuzzy Control of Nonlinear Systems", *IEEE Trans. on Fuzzy Systems*, pp. 146-155.

Appendix A: Membership Definitions

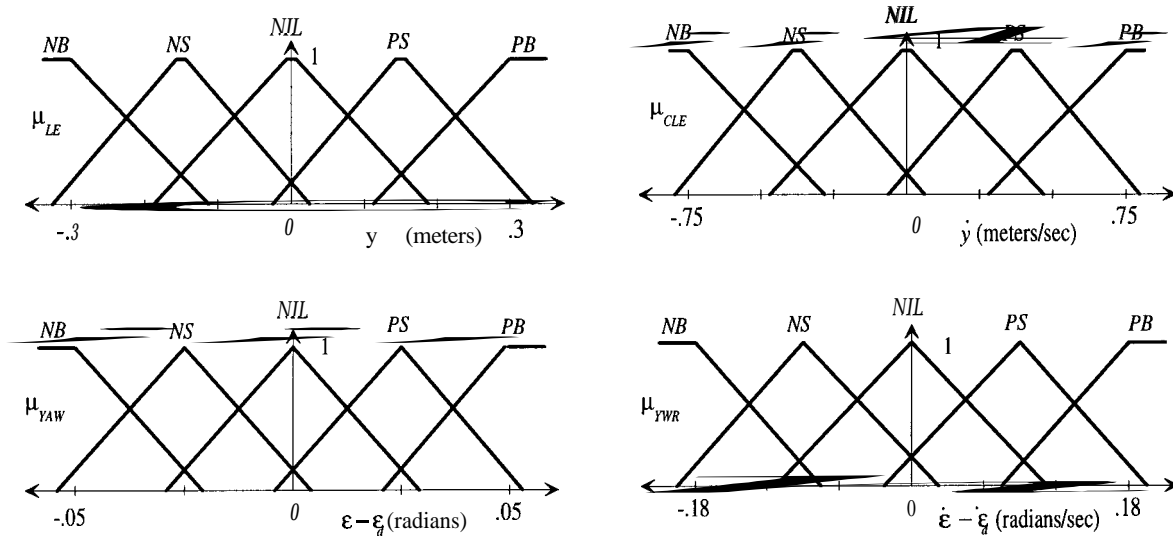


Figure A.1: Membership Functions, μ for x

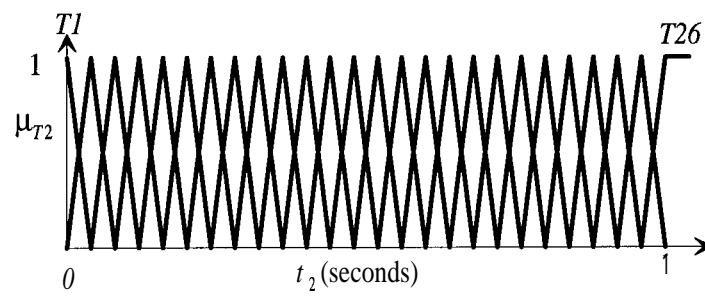


Figure A.2: Membership Functions, μ , for t_2

Appendix B: Linear Model of Vehicle

The *linear* model is derived by linearizing the nonlinear model [15], retaining only the motions of lateral translation and yaw rotation. The required assumptions are as follows:

1. the roll, ϕ , and pitch, θ , rotational motions and the vertical, z , translational motion can be neglected,
2. the longitudinal velocity, v_x , of the vehicle is constant,
3. the side slip angle, β , and error in yaw angle, $\epsilon - \epsilon_d$, is small (note that ϵ_d is dependent on the road geometry, and
4. the super elevation, γ , and gradient, A , angles in the roadway are small.

Figure B.1 shows the schematic of the linear model of the vehicle relative to the reference roadway.

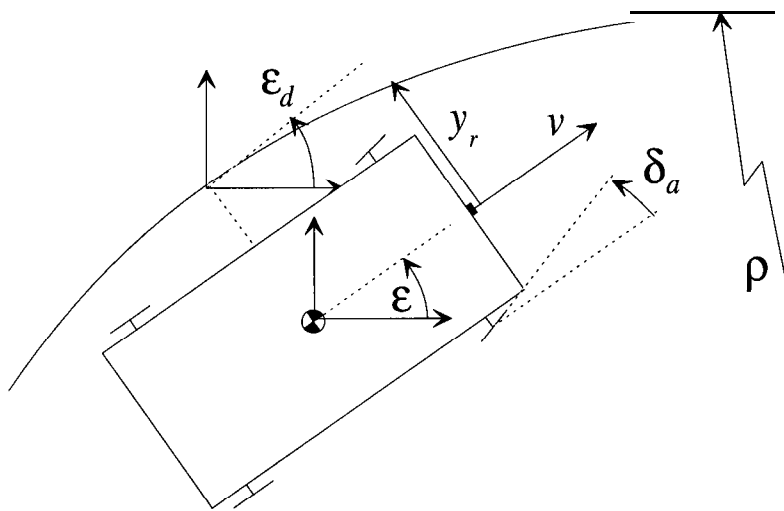


Figure B.1: Schematic of the Linear Model

The nomenclature for the linear model is reduced to the following:

y_r :	lateral displacement of the vehicle c.g. from center of road
ε :	yaw angle displacement of the unsprung mass of the vehicle
ε_d :	desired yaw angle displacement of the vehicle, set by the road reference
v_x :	vehicle speed in the longitudinal direction
ρ :	radius of curvature of the road
δ_a :	actual front wheel steering angle
m :	mass of the vehicle
I_z :	moment of inertia of the sprung mass in the z direction
$l_1, (l_2)$:	distance from the c.g. to the front (rear) axle
$C_{sf}, (C_{sr})$:	cornering stiffness of the front (rear) tires

The linear model can be expressed as a fourth order equation in state space form as follows:

$$\frac{d}{dt} \begin{bmatrix} y_r \\ \dot{y}_r \\ \varepsilon - \varepsilon_d \\ \dot{\varepsilon} - \dot{\varepsilon}_d \end{bmatrix} = \begin{bmatrix} 0 & 1 & 0 & 0 \\ 0 & A_1/v & -A_1 & A_2/v \\ 0 & 0 & 0 & 1 \\ 0 & A_3/v & -A_3 & A_4/v \end{bmatrix} \begin{bmatrix} y_r \\ \dot{y}_r \\ \varepsilon - \varepsilon_d \\ \dot{\varepsilon} - \dot{\varepsilon}_d \end{bmatrix} + \begin{bmatrix} 0 \\ B_1 \\ 0 \\ B_2 \end{bmatrix} \delta_a + \begin{bmatrix} 0 \\ A_2 - v^2 \\ 0 \\ A_4 \end{bmatrix} \frac{1}{\rho},$$

where

$$A_1 = \frac{-2(C_{sf} + C_{sr})}{m}, \quad A_2 = \frac{2(l_2 C_{sr} - l_1 C_{sf})}{m},$$

$$A_3 = \frac{2(l_2 C_{sr} - l_1 C_{sf})}{I_z}, \quad A_4 = \frac{-2(l_2^2 C_{sr} + l_1^2 C_{sf})}{I_z},$$

$$B_1 = \frac{2C_{sf}}{m}, \text{ and} \quad B_2 = \frac{2l_1 C_{sf}}{I_z}.$$